



HAL
open science

Phytoplankton pigment distribution in relation to upper thermocline circulation in the eastern Mediterranean Sea during winter

Francesca Vidussi, Hervé Claustre, Beniamino B Manca, Anna Luchetta,
Jean-Claude Marty

► To cite this version:

Francesca Vidussi, Hervé Claustre, Beniamino B Manca, Anna Luchetta, Jean-Claude Marty. Phytoplankton pigment distribution in relation to upper thermocline circulation in the eastern Mediterranean Sea during winter. *Journal of Geophysical Research. Oceans*, 2001, 106 (C9), pp.19939-19956. 10.1029/1999JC000308 . insu-03325437

HAL Id: insu-03325437

<https://insu.hal.science/insu-03325437>

Submitted on 24 Aug 2021

HAL is a multi-disciplinary open access archive for the deposit and dissemination of scientific research documents, whether they are published or not. The documents may come from teaching and research institutions in France or abroad, or from public or private research centers.

L'archive ouverte pluridisciplinaire **HAL**, est destinée au dépôt et à la diffusion de documents scientifiques de niveau recherche, publiés ou non, émanant des établissements d'enseignement et de recherche français ou étrangers, des laboratoires publics ou privés.

Copyright

Phytoplankton pigment distribution in relation to upper thermocline circulation in the eastern Mediterranean Sea during winter

Francesca Vidussi¹, Hervé Claustre¹, Beniamino B. Manca², Anna Luchetta³, and Jean-Claude Marty¹

Abstract. Using a sampling grid of 67 stations, the influence of basin-wide and subbasin-scale circulation features on phytoplankton community composition and primary and new productions was investigated in the eastern Mediterranean during winter. Taxonomic pigments were used as size class markers of phototroph groups (picophytoplankton, nanophytoplankton and microphytoplankton). Primary production rates were computed using a light photosynthesis model that makes use of the total chlorophyll *a* (Tchl *a*) concentration profile as an input variable. New production was estimated as the product of primary production by a pigment-based proxy of the *f* ratio (new production/total production). For the whole eastern Mediterranean, Tchl *a* concentration was 20.4 mg m^{-2} , and estimated primary and new production were 0.27 and $0.04 \text{ g C m}^{-2} \text{ d}^{-1}$, respectively, when integrated between the surface and the depth of the productive zone (1.5 times the euphotic layer). Nanophytoplankton and picophytoplankton (determined from the pigment-derived criteria) were the dominant size classes and contributed to 60 and 27%, respectively, of Tchl *a*, while microphytoplankton contributed only to 13%. Subbasin and, to a certain extent, mesoscale structures (cyclonic and anticyclonic gyres) were exceptions to this general trend. Anticyclonic gyres were characterized by low Tchl *a* concentrations ($18.8 \pm 4.2 \text{ mg m}^{-2}$, with the lowest value being 12.4 mg m^{-2}) and the highest picophytoplankton contribution (40% of Tchl *a*). In contrast, cyclonic gyres contained the highest Tchl *a* concentration ($40.3 \pm 15.3 \text{ mg m}^{-2}$) with the highest microphytoplankton contribution (up to 26% of Tchl *a*). Observations conducted at a mesoscale in the Rhode gyre (cyclonic) region show that the core of the gyre is dominated by microphytoplankton (mainly diatoms), while adjacent areas are characterized by high chlorophyll concentration dominated by picophytoplankton and nanophytoplankton. We estimate that the Rhodes gyre is a zone of enhanced new production, which is 9 times higher than that in adjacent oligotrophic areas of the Levantine basin. Our results confirm the predominance of oligotrophic conditions in the eastern Mediterranean and emphasize the role of subbasin and mesoscale dynamics in driving phytoplankton biomass and composition and, finally, biogeochemical cycling in this area.

1. Introduction

It is recognized that physical processes affect the structure of plankton communities [Legendre and Demers, 1984; Mann and Lazier, 1991]. Water movements, such as eddies and jets, may cause vertical mixing, which can enhance nutrient transport from deeper water masses to surface layers [Legendre and Demers, 1984]. This availability of "new nutrients" enhances phytoplankton biomass and production [e.g., Lohrenz et al., 1993; Claustre et al., 1994]. Exogenous nitrates are principally used by large phytoplankton (microphytoplankton),

which mainly contribute to new production [Goldman, 1993], while regenerated forms of nitrogen (ammonium and urea) are the likely source for small phytoplankton (picophytoplankton and nanophytoplankton). Therefore the input of new nutrients in the euphotic layer is expected to modify the composition of the phytoplankton community. On the basis of the size of the primary producers, two types of food web pathways can be distinguished [Legendre and Rassoulzadegan, 1995]: (1) the herbivorous food web, based on large phytoplankton, herbivorous zooplankton, and fish, and (2) the microbial food web, which consists of small phytoplankton, heterotrophic bacteria, and protozoa. Food web structure controls the fate of biogenic carbon such that export of particulate organic matter occurs when large phytoplankton and the herbivorous food chain dominate, whereas the microbial food web leads to recycling and to weak exportation of organic material [Michaels and Silver, 1988]. Therefore hydrodynamics can affect the magnitude and composition of phytoplankton biomass, the structure of the food web, and the balance between exported and recycled production [Legendre and LeFevre, 1989].

The influence of hydrodynamic forcing on phytoplankton community structure may occur at different spatial scales that

¹Observatoire Océanologique de Villefranche, Laboratoire d'Océanographie de Villefranche, Université Pierre et Marie Curie and CNRS/INSU, Villefranche-sur-mer, France.

²Istituto Nazionale di Oceanografia e Geofisica Sperimentale, Trieste, Italy.

³Istituto Talassografico, Trieste, Italy.

Copyright 2001 by the American Geophysical Union.

Paper number 1999JC000308.
0148-0227/01/1999JC000308\$09.00

range from a few meters (e.g., the mixed layer depth) to thousands of kilometers (basin scale). Given our present observation capabilities, this makes the observation of such an influence a challenge for most oceanic areas. Remote sensing can resolve large and mesoscale patterns but not phytoplankton community structure. On the other hand, discrete sampling allows phytoplankton community structure to be characterized but not simultaneously over a large range of spatial scales.

The eastern Mediterranean is a relative small basin, which allows quasi-synoptic resolution of variability on different spatial scales and possesses hydrodynamic processes that are quite similar to those observed in the open ocean [POEM group, 1992]. Therefore this basin may serve as an interesting case study [Béthoux and Gentili, 1994; Malanotte-Rizzoli et al., 1996] to investigate the influence of hydrodynamics on phytoplankton community composition and subsequent effects on biogeochemical cycling. In addition, as the euphotic layer of the eastern Mediterranean Sea is nutrient-depleted throughout most of the year, this basin is considered as one of the most oligotrophic areas of the world's oceans [Berman et al., 1986]. Moreover, superimposed on this general oligotrophic character, episodic blooms and elevated levels of primary production related to specific hydrographic features have been reported in field studies or detected through Coastal Zone Color Scanner (CZCS) imagery [Salihoglu et al., 1990; Krom et al., 1992; Antoine et al., 1995].

The aims of the present study, conducted in the eastern Mediterranean Sea during winter as part of *Meteor* cruise 31/1, were (1) to provide evidence for the influence of various circulation features (from basin-scale to meso-scale) on phytoplankton community structure using high-performance liquid chromatography (HPLC)-determined pigment biomarkers and (2) to address the relationships between phytoplankton community structure and the balance between regenerated and new production in the various identified circulation features using a combination of pigment information and a light photosynthesis model.

2. Methods

2.1. Water Sampling and Analysis

2.1.1. Hydrographic measurements and water sample collection. The basin-wide *Meteor* cruise 31/1 (December 30, 1994 to February 5, 1995) was part of both the Physical Oceanography of the Eastern Mediterranean-Biological Chemical (POEM-BC) and the Marine Science and Technology-Mediterranean Targeted Project (MAST-MTP) programs. Temperature and salinity vertical profiles (surface to 250-330 m) were measured at 69 stations (Figure 1) in the eastern Mediterranean Sea using a SeaBird SBE-911 plus conductivity-temperature-depth profiler (CTD) equipped with a Sea Teach fluorometer. Quality control CTD data were obtained with parallel Neil Brown MK3 CTD deep casts. The salinity and temperature data were routinely checked against independent measurements performed on board with a Guildline 8400 salinometer (accuracy ± 0.002) and digital SIS reversing thermometer readings (resolution $\pm 0.001^\circ\text{C}$), respectively. Water samples for nitrates and pigments were collected using a rosette Niskin bottle system at 69 and 67 stations, respectively, and at 12 shallow depths, which were selected by examining the fluorometer profiles obtained during the downcast.

2.1.2. Nutrient and pigment analysis. Nutrient (nitrate and nitrite) samples were collected in acid-washed 50 mL po-

lypropylene bottles. Nitrate plus nitrite and nitrite were analyzed on board within a few hours after recovery of the rosette, or frozen until analysis, using a Technicon Auto-analyzer II according to the procedures described by Grasshoff [1983]. Precision of the method, calculated from five replicates, was $\pm 0.04 \mu\text{M}$ (Cv < 5.0%). Nitrate concentrations were obtained subtracting nitrite from nitrate plus nitrite concentrations. The depth of the nitracline (Z_n) was calculated as the depth of the center of the gradient of the NO_3 profile.

For pigment analysis, 2-4 L of seawater were filtered through 25 mm GF/F Whatman glass fiber filters. The filters were stored in liquid nitrogen until the end of the cruise and then frozen (-20°C) until analysis. Samples were extracted in 3 mL methanol, which contained a known amount of the internal standard Zn(II) pyropheophorbide *a* octadecyl ester [Mantoura and Repeta, 1997]. Pigment extracts were stored for 1 hour at -20°C sonicated with a sonication probe, and subsequently, filtered onto 25 mm GF/C Whatman glass fiber filters. Pigments were analyzed by HPLC using the method and chromatographic system (augmented with a Thermo Separation Products Autosampler AS3000) described by Vidussi et al. [1996]. The Autosampler mixed 800 μL of extract with 400 μL of 1 M ammonium acetate before injection through a 500 μL loop onto a 3 μm C8 column (Hypersil® endcapped MOS, 10 cm, 4.6 mm ID, Shandon). Pigments (chlorophylls and carotenoids) were detected and quantified using a variable wavelength Milton Roy detector set to 440 nm. Pigments were identified using an on line diode array detector (Waters 991) on selected samples. The HPLC system was calibrated using a chlorophyll *a* standard (Sigma) and chlorophyll and carotenoid standards as recommended by Scientific Committee on Research, U. N. Educational, Scientific, and Cultural Organisation (UNESCO) [Repeta and Bjørnland, 1997].

2.2. Data Processing and Analysis

2.2.1. Hydrographic measurements. The CTD data were collected at a maximum rate of 24 scans s^{-1} . Throughout this paper, pressure is used as the vertical coordinate, temperature is given as potential temperature θ , and salinity is according to the practical salinity scale. The dynamical computations are based on a reference level of 800 dbar, which corresponds approximately to the bottom of the Levantine Intermediate Water layer [Malanotte-Rizzoli et al., 1997]. The dynamic height anomalies are calculated in $\text{m}^2 \text{s}^{-2}$ in reference to 800 dbar and depicted subtracting the mean from the computed values. The objective analyses are made on a regular grid spaced over $1/4^\circ$ using an isotropic correlation function fitted to observations after first order polynomial detrending. The first zero crossing was typically of the order of 180-200 km, and the decay scale was reduced by a factor of $\sqrt{2}$ [Carther and Robinson, 1987]. The field was not represented when the normalized error exceeded 60%. From an examination of station distributions (Figure 1), a detailed identification of the horizontal circulation structures cannot be made. Only the interconnecting basin-scale jet-like currents and the coarser elements of subbasin-scale features can be revealed. Features with mesoscale and submesoscale signatures, i.e., those with dimensions of 2 or 3 times the internal Rossby radius of deformation, calculated of the order of 10-12 km [POEM Group, 1992], can be revealed from the satellite IR image traced by the monthly average sea surface temperature (SST) over the period immediately before the cruise (see section 3). However, the near-surface vertical distribution of temperature and salinity, plotted along the sec-

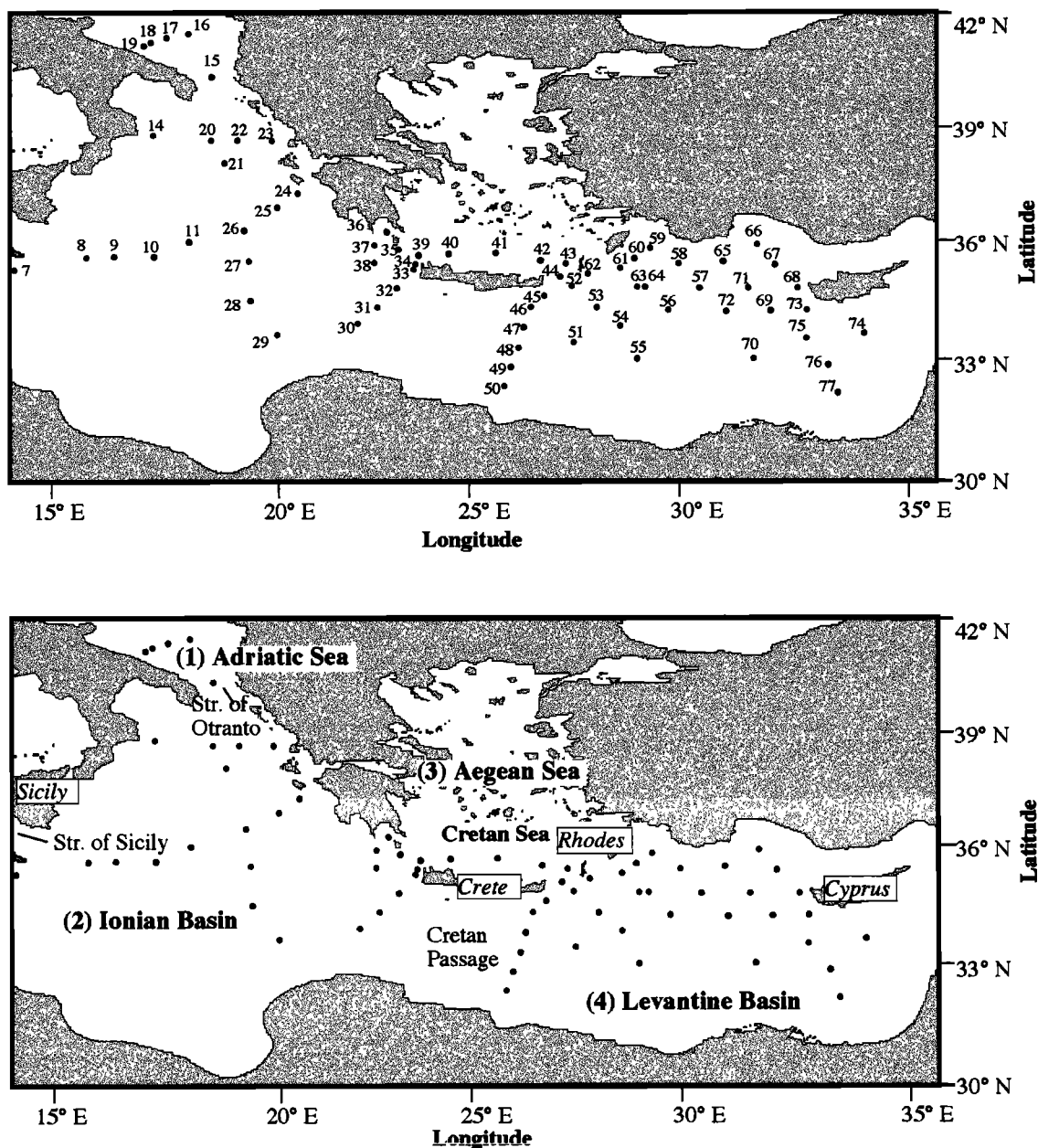


Figure 1. (top) Location of stations sampled during *Meteor* cruise 31/1 between January and February 1995 in the eastern Mediterranean Sea. (bottom) Map of the investigated area with geographical provinces.

tions crossing the gyres, aid the interpretation of the water mass pathways observed in the horizontal analysis (see section 3). The mixed layer depth Z_{ml} was defined as the deepest depth where the potential density does not exceed surface (2.5 dbar) density by a given threshold. Thresholds of 0.01, 0.02, 0.03, 0.04, and 0.05 were examined. In 90% of the cases the 0.01 criterion was retained.

2.2.2. Taxonomic pigments and size structure indices.

The chemotaxonomic correspondence of HPLC-determined pigments (Table 1) can be used to study the phytoplankton community composition [e.g., *Gieskes et al.*, 1988; *Goericke and Repeta*, 1993; *Claustre and Marty*, 1995]. With the increasing capacity of HPLC techniques (reduction of the analysis time and automation), pigment databases are generally large (e.g., 804 samples in this study). Moreover, some pigments may covary with others or be redundant, which can

make data interpretation and visualization tedious. Therefore data reduction is required in order to extract the relevant information, especially for a purpose of comparison with the major patterns of hydrography. Furthermore, from a biogeochemical point of view the size structure of phytoplankton communities is a more appropriate parameter than the community composition itself. Small phytoplankton are generally associated with nutrient-depleted oligotrophic waters, while large phytoplankton predominate in nutrient-rich and productive systems. Therefore pigment data reduction was performed with this aim in mind using the size taxonomic pigment correspondence presented in Table 1.

The diagnostic pigments (DP, in mg m^{-3} or in mg m^{-2}) are defined as the sum of seven diagnostic pigments:

$$\text{DP} = \text{Zea} + \text{Tchl } b + \text{Allo} + 19' \text{-HF} + 19' \text{-BF} + \text{Fuco} + \text{Peri}. \quad (1)$$

Table 1. Taxonomic Pigments Used in This Study and Their Significance in Term of Size Class

Pigments	Abbreviations	Taxonomic Significance	Size μm	References ^a
Zeaxanthin	Zea	cyanobacteria and prochlorophytes	< 2	1, 2, 5
Divinyl-chlorophyll <i>a</i>	Dv-chl <i>a</i>	prochlorophytes	< 2	3, 4, 5
Chlorophyll <i>b</i> +Divinyl-chlorophyll <i>b</i>	Tchl <i>b</i>	green flagellates and prochlorophytes	< 2	6, 7, 8, 9
19' hexanoyloxyfucoxanthin	19'-HF	chromophytes nanoflagellates	2-20	10, 11, 12, 13, 14
19' butanoyloxyfucoxanthin	19'-BF	chromophytes nanoflagellates	2-20	10, 13, 14, 15, 16
Alloxanthin	Allo	cryptophytes	2-20	14, 17
Fucoxanthin	Fuco	diatoms	> 20	10, 11, 13, 18
Peridinin	Peri	dinoflagellates	> 20	18, 19, 20

^aReferences are 1, Gieskes *et al.* [1988]; 2, Guillard *et al.* [1985]; 3, Goericke and Repeta [1992]; 4, Gieskes and Kraay [1983a]; 5, Chisholm *et al.* [1988]; 6, Partensky *et al.* [1993]; 7, Moore *et al.* [1995]; 8, Jeffrey [1976]; 9, Simon *et al.* [1994]; 10, Bjørnland and Liaaen-Jensen [1989]; 11, Hooks *et al.* [1988]; 12, Arpin *et al.* [1976]; 13, Wright and Jeffrey [1987]; 14, Jeffrey and Vesik [1997]; 15, Andersen *et al.* [1993]; 16, Bjørnland *et al.* [1989]; 17, Gieskes and Kraay [1983b]; 18, Kimor *et al.* [1987]; 19, Johansen *et al.* [1974]; and 20, Jeffrey *et al.* 1975.

The prochlorophyte marker divinyl (DV)-chl *a* (Table 1) is not included in DP as zeaxanthin is a marker of surface prochlorophyte populations (together with cyanobacteria) and Tchl *b* is a marker of deep prochlorophyte populations (together with green flagellates). Figure 2 shows that water column-integrated (0-300 m) total chlorophyll *a* (Tchl *a*) concentration is linearly related to integrated DP (linear regression was calculated using the model II geometric mean method). The relationship is significant ($r=0.97$, $n=67$, and $p<0.001$), which makes DP a valid estimator of Tchl *a*. We assume that each diagnostic pigment contributes equally to chlorophyll *a* (chl *a*), an assumption that is not strictly realistic since diagnostic pigment/chl *a* ratios may vary with species and physiological state [e.g., Kana and Glibert, 1987]. Nevertheless, this assumption is reasonable for mapping purposes and interpretation of general trends on a large-scale basis.

The biomass proportion (BP) associated with each size class is further defined as

$$\text{BP}_{\text{pico}} = (\text{Zea} + \text{Tchl } b) / \text{DP}, \quad (2)$$

$$\text{BP}_{\text{nano}} = (\text{Allo} + 19'\text{-HF} + 19'\text{-BF}) / \text{DP}, \quad (3)$$

$$\text{BP}_{\text{micro}} = (\text{Fuco} + \text{Peri}) / \text{DP}, \quad (4)$$

where the subscripts pico, nano, and micro refer to the size classification of Sieburth *et al.* [1978]: picophytoplankton (<2 μm), nanophytoplankton (2-20 μm), and microphytoplankton (20-200 μm).

The pigment-derived classes defined here do not strictly refer to the true size of phytoplankton as can be the case for studies based on chlorophyll size fraction. In particular, diatoms (fucoxanthin) and dinoflagellates (peridinin) are associated here with microphytoplankton, which is not always the rule (e.g., diatoms <20 μm have been reported in the tropical Pacific by Chavez *et al.* [1996]). Although studies focused on phytoplankton size in the eastern Mediterranean are scarce, the investigation of Kimor *et al.* [1987] off the coast of Israel (eastern Mediterranean Sea) reported that large (>65 μm) diatoms and dinoflagellates dominate the community (more than 90% of the cell number). This observation is at least a partial validation of the pigment-derived size class BP_{micro} . Note that BP_{micro} is equivalent to the Fp ratio [Claustre, 1994], defined as the biomass ratio of phytoplankton involved in new production over total phytoplankton, and, as such, is a proxy of the *f* ratio (new production/total production) [Eppley and Peterson, 1979]. This means that together with a size signifi-

cance, some of the criteria defined, also have a functional/biogeochemical significance.

Finally, the average ($n=804$) pigment composition within each class determined from the pigment-derived criteria was as follows: (1) picophytoplankton (zea+Tchl *b*) were composed of 52% of zeaxanthin, 33% of chlorophyll *b*, and 15% of divinyl-chlorophyll *b*; (2) nanophytoplankton (19'-HF+19'-BF+Allo) were composed of 68% of 19'-HF, 29% of 19'-BF, and 3% of alloxanthin; and (3) microphytoplankton (Fuco+Peri) were composed of 82% of fucoxanthin and 18% of Peridinin.

Integrated Tchl *a* ($\Sigma\text{Tchl } a$ in $\text{mg chl } a \text{ m}^{-2}$) was computed for the 0-1.5 Z_e layer (hereafter called the "productive layer") where Z_e corresponds to the euphotic depth defined as the depth where the photosynthetically available radiation (PAR) is reduced to 1% of its surface value. Z_e was estimated using the model described by Morel [1988] on the measured HPLC-Tchl *a* profile. The chl *a* associated with each size class (in $\text{mg chl } a \text{ m}^{-2}$) is subsequently computed as the product of BP and

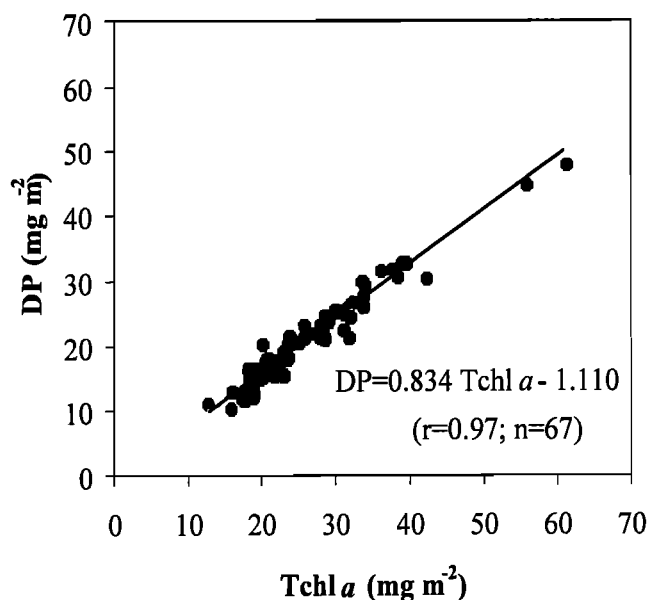


Figure 2. Relationship between water column-integrated (0-300 m) concentrations of Tchl *a* and DP.

Tchl a , both integrated down to $1.5 Z_e$:

$$\Sigma \text{pico chl } a = \text{BP}_{\text{pico}} \Sigma \text{Tchl } a, \quad (5)$$

$$\Sigma \text{nano chl } a = \text{BP}_{\text{nano}} \Sigma \text{Tchl } a, \quad (6)$$

$$\Sigma \text{micro chl } a = \text{BP}_{\text{micro}} \Sigma \text{Tchl } a. \quad (7)$$

2.2.3. Computation of primary and new production.

Primary production was computed according to the spectral photosynthesis model of *Morel* [1991]. This model first employs an atmospheric segment, which computes, for each day and a given latitude, the spectral irradiance at the ocean surface for a clear sky. The biooptical segment of this model, which is based on standard parameters of algal physiology [*Morel et al.*, 1996], predicts the vertical profile of daily primary production from measured Tchl a profile and measured temperatures. The same algal physiological parameters [*Morel et al.*, 1996, table 1, version 2] were employed here; however, no attempt was made to account for the possible dependence of physiological parameters on community composition in the computation of primary production. Estimates of modeled primary production calculated in this study were not compared to field measurements, and no sensitivity analysis of the model was possible because ^{14}C primary production rates were not measured during *Meteor* cruise 31/1. Integrated primary production (ΣPP , in $\text{g C m}^{-2} \text{d}^{-1}$) was computed down to $1.5 Z_e$. Subsequently, the integrated new production (ΣNP , in $\text{g C m}^{-2} \text{d}^{-1}$) was defined as

$$\Sigma\text{NP} = \text{BP}_{\text{micro}} \Sigma\text{PP}. \quad (8)$$

Similarly, regenerated production (ΣRP , in $\text{g C m}^{-2} \text{d}^{-1}$) was defined as

$$\Sigma\text{RP} = (1 - \text{BP}_{\text{micro}}) \Sigma\text{PP}. \quad (9)$$

According to previous studies that report that principally large phytoplankton (e.g., diatoms) are involved in new production [e.g., *Goldman*, 1993; *Villareal et al.*, 1999] the new production computed here takes into account only the contribution of microphytoplankton (diatoms and dinoflagellates). Therefore

this new production may be an underestimate when N_2 fixing cyanobacteria are abundant and in the case when algae other than diatoms or dinoflagellates (e.g., prymnesiophytes) contribute significantly to new production.

3. Results

3.1. Whole Eastern Basin

The dynamic height anomaly at the surface with reference to 800 dbar (Figure 3) essentially shows the most significant features of the upper thermocline general circulation (for nomenclature, see *Robinson et al.* [1991], *Ozsoy et al.* [1993], and *Theocharis et al.* [1993]). In winter 1995 the general circulation shows a near-surface current that, entering through the Sicily Strait (Figures 3 and 4), meanders into the northern Ionian transporting Modified Atlantic Water (MAW). The major branch of the current turns southward and veers to the east upon entering the Cretan passage (south of Crete) where it rejoins the Mid-Mediterranean Jet (MMJ) transporting MAW into the Levantine basin. The satellite image (Plate 1a) indicates warm surface water along the coastal regions, which is up to 6°C higher than cold patches located within the basin interior. A tendency for general anticyclonic rotation is evident (Plate 1a; e.g., in the Ionian interior and along the African coast) and is associated with low surface layer nitrate concentrations (generally $<0.5 \mu\text{M}$ and sometimes undetectable; Plate 1b), except in some peculiar situations (see later). At the same time, Tchl a concentrations integrated over the 0-1.5 Z_e layer ($\Sigma\text{Tchl } a$) were low ($12.6\text{--}33.5 \text{ mg chl } a \text{ m}^{-2}$; Plate 1c). Among the different phytoplankton classes (determined from the pigment-derived criteria) the microphytoplankton biomass showed the largest variability (from 0.9 to $11.8 \text{ mg chl } a \text{ m}^{-2}$) as compared to nanophytoplankton (from 7.3 to $21.5 \text{ mg chl } a \text{ m}^{-2}$) and picophytoplankton biomasses (from 3.3 to $9.7 \text{ mg chl } a \text{ m}^{-2}$; Plate 2). Nevertheless, nanophytoplankton was the dominant algal size class (Table 2). The integrated primary

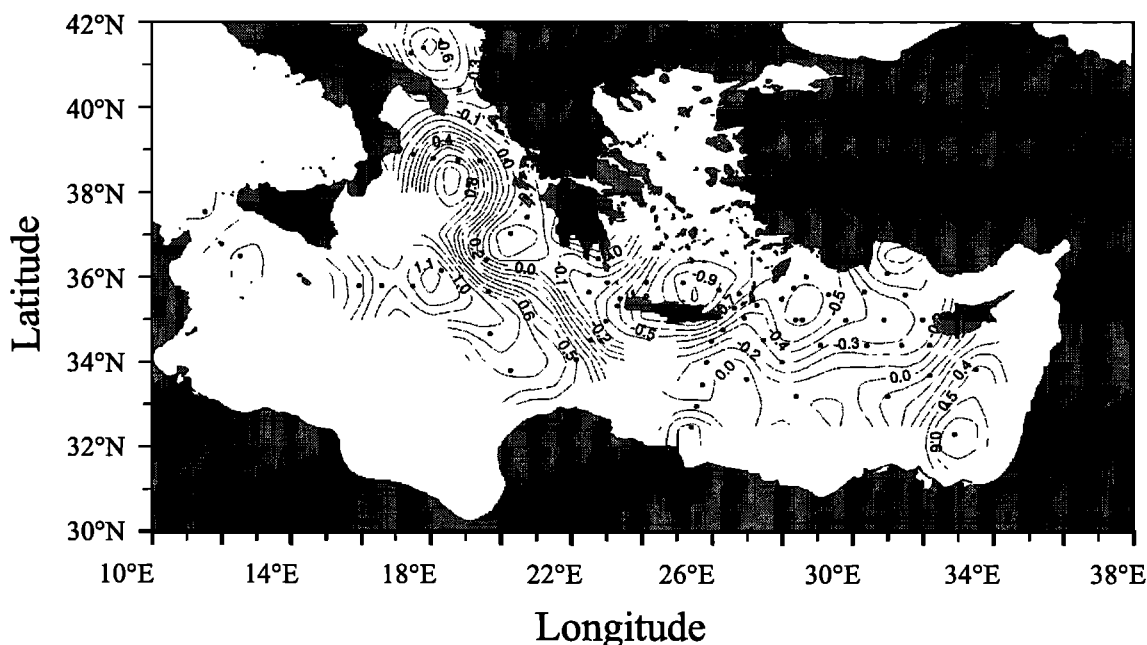


Figure 3. Dynamic height anomalies (m^2s^{-2}) at the surface with reference to 800 dbar during the *Meteor* cruise 31/1 (January 1995). The network of CTD stations is marked by dots.

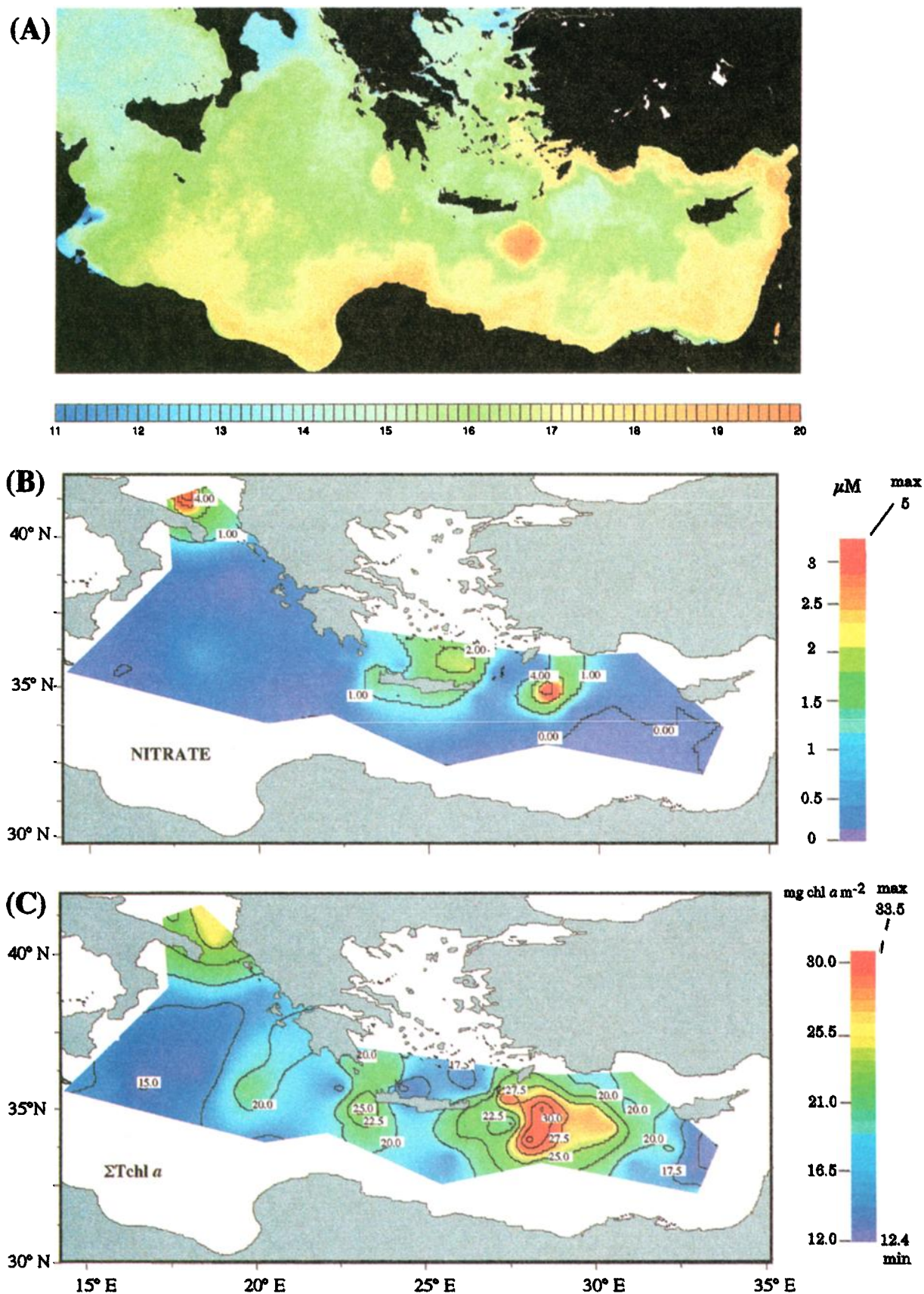


Plate 1. (a) Satellite image of monthly averaged SST (December 1994) and distribution of (b) nitrate concentrations at 10 m and (c) $\Sigma\text{Tchl } a$ concentrations in the eastern Mediterranean Sea during winter. Data of satellite image are courtesy of Deutsche Forschungsanstalt für Luft-und Raumfahrt e.V., reprocessed at OGS, Trieste, Italy, by C. Fragiaco.

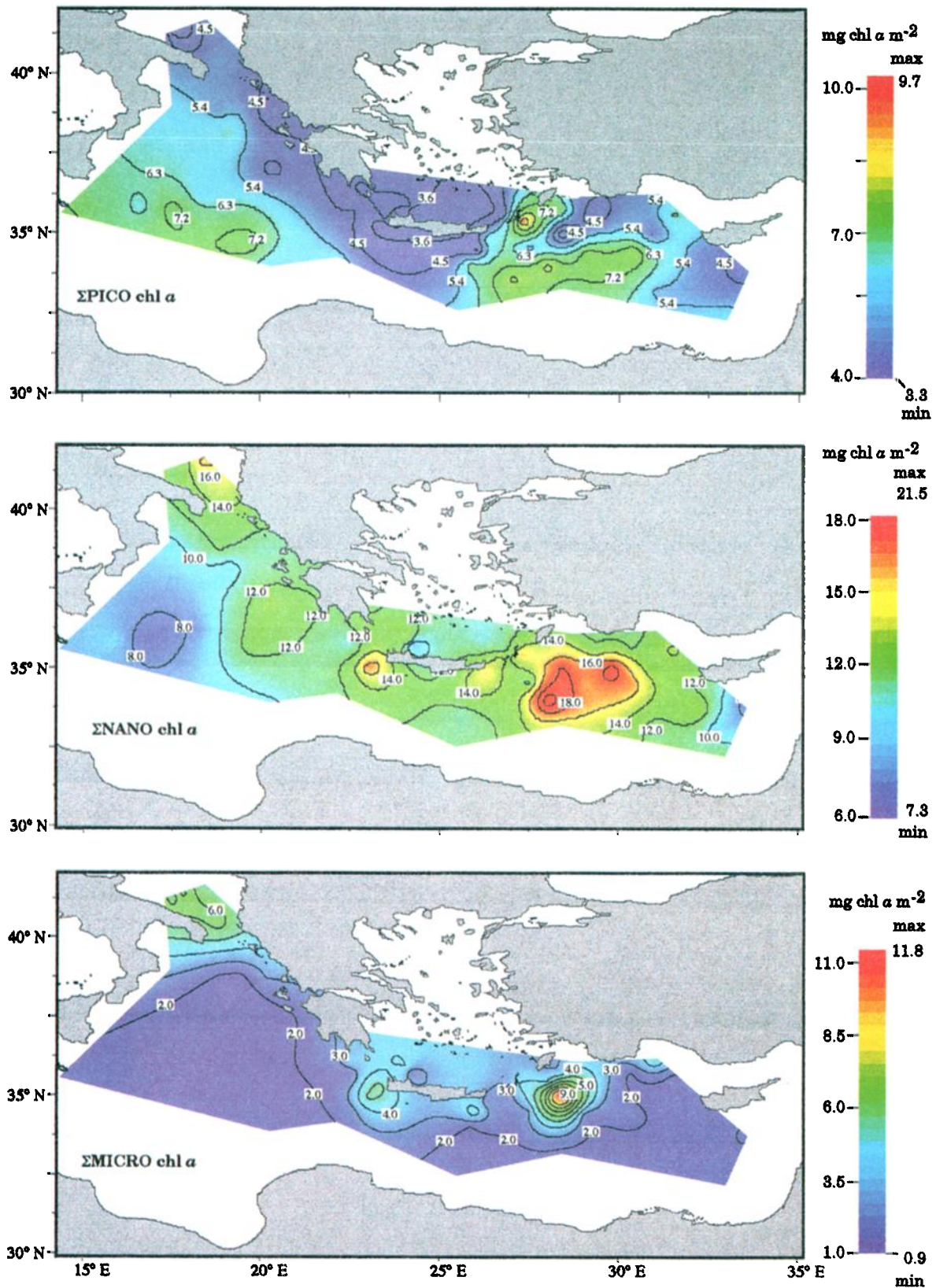


Plate 2. Distribution of (top) ΣPICO chl *a*, (middle) ΣNANO chl *a*, and (bottom) ΣMICRO chl *a* concentrations in the eastern Mediterranean Sea during winter.

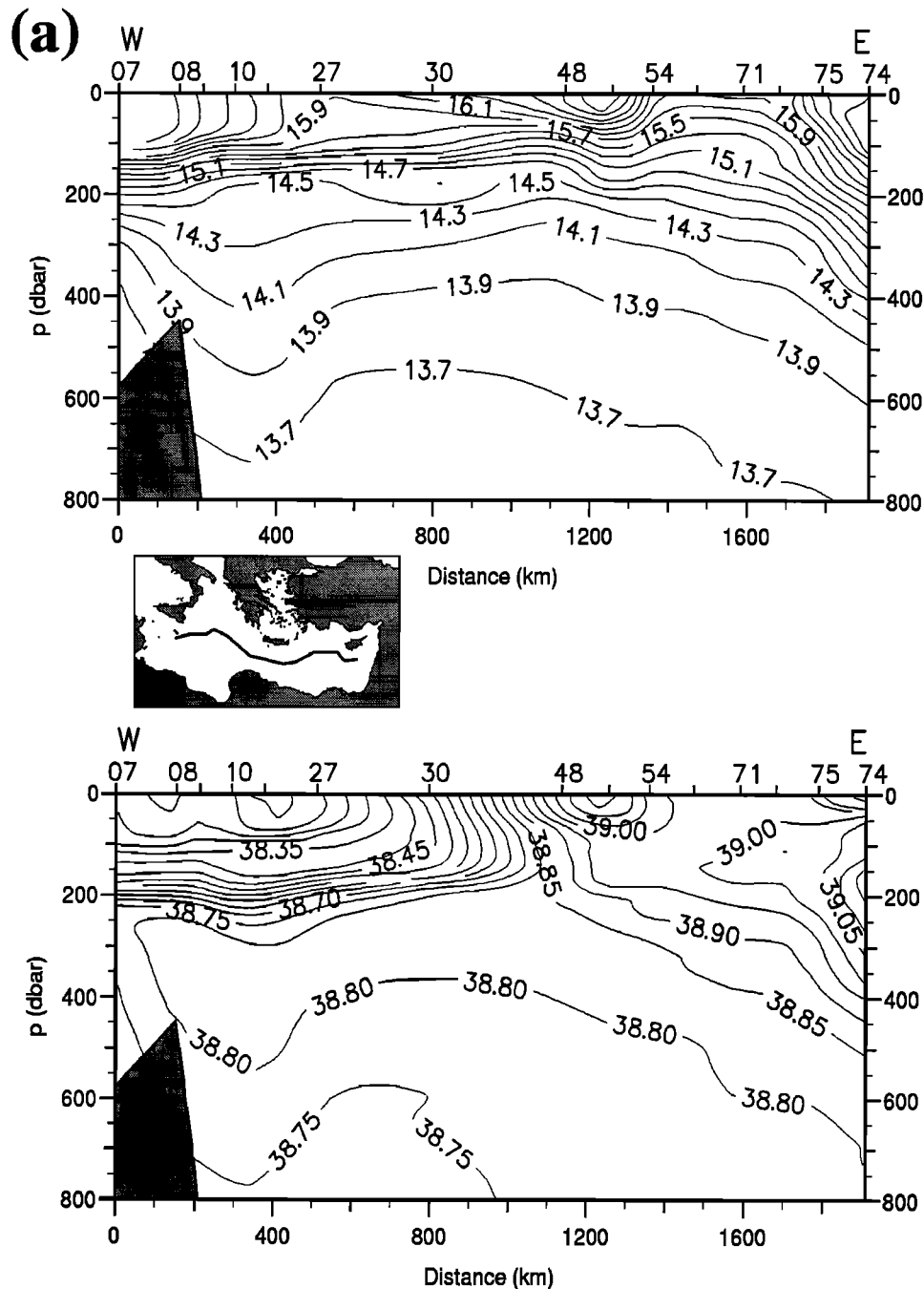


Figure 4. Vertical distributions of (top) temperature and (bottom) salinity down to 800 dbar (a) for the cross section through the eastern Mediterranean (see insert map), (b) for the cross section in the Ionian (see insert map), and (c) for the cross section in the Levantine basin (see insert map). The numbers at the top axis indicate the station positions along the section.

production rates ranged from 0.17 to 0.42 $\text{gC m}^{-2} \text{d}^{-1}$ (Plate 3). Integrated new production rates were variable and ranged over more than one order of magnitude (from 0.01 to 0.15 $\text{gC m}^{-2} \text{d}^{-1}$; Plate 3). The Tchl *a* concentrations were quasi-homogeneously distributed in the euphotic layer, and surface values varied between 0.090 and 0.485 mg m^{-3} (Figure 5). Phytoplankton class concentrations and estimated productions (NP and RP), when plotted against nitrate concentrations integrated over the productive layer ($\Sigma\text{nitrate}$, Figure 6), showed different linear relationships: microphytoplankton was positively correlated ($p < 0.001$, $r = 0.66$, and $n = 64$) with $\Sigma\text{nitrate}$ concentrations,

while the reverse was observed for picophytoplankton ($p < 0.001$, and $r = 0.62$). In contrast, no relationship was observed between nitrate and nanophytoplankton. Finally, nitrate concentrations were positively correlated with new production ($p < 0.001$ and $r = 0.63$), while no significant relationship was observed between nitrate and regenerated production ($r = 0.13$).

3.2. Regional Oceanography

The geographical regions (Figure 1) were analyzed separately on the basis of their hydrographic properties and dynamics and their effect on chemical and biological response,

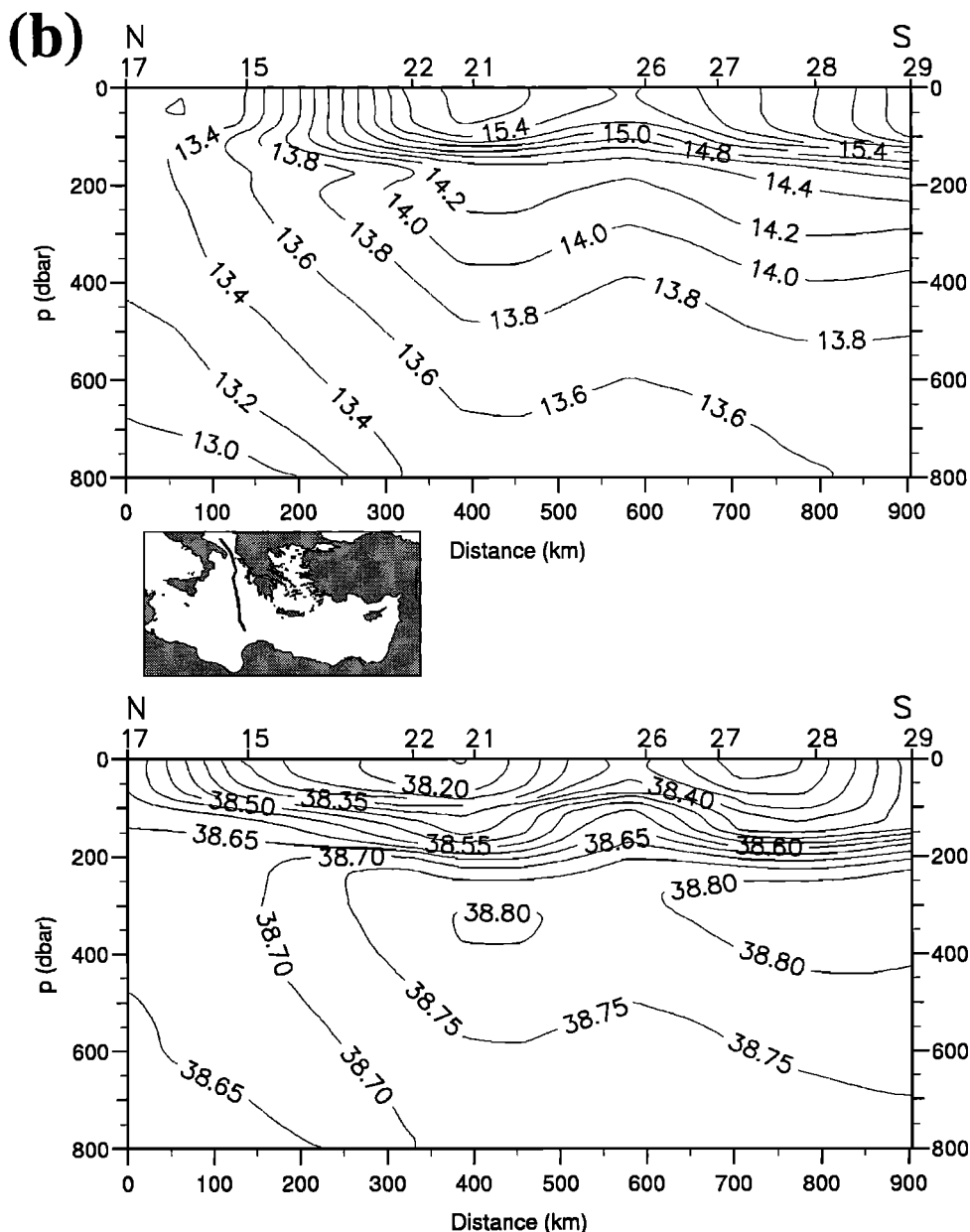


Figure 4. (continued)

namely, the Adriatic Sea, the Ionian basin, the Aegean Sea, and the Levantine basin. In addition to the continuous current system described above, the eddy field provides evidence for some local structures, which partially define the former system and which have been described in detail in the geographical region sections. Since some structures (e.g., the intense Ierapetra anticyclone to the southeast of Crete, Plate 1a) were not adequately covered by the station network, only the well covered structures have been described in detail.

3.2.1. Adriatic Sea. The southern portion of the Adriatic Sea is characterized by cyclonic circulation (Figure 3). Colder and saltier water of Levantine origin intrudes into the Adriatic Sea in the intermediate layer and upwells in the center of the gyre. The cyclonic vorticity is generally defined by the outcropping of the isotherm 13.3°C and isohaline 38.60 at station 17. Here the dynamics mixed the upper 250 m (Figure 4) and upwelled nitrate-rich water (5 μ M) in the euphotic layer (Plate 1b). In response to the upwelling of nitrate-rich waters, rela-

tively high concentrations in $\Sigma Tchl a$ (24.1 ± 2.3 mg chl a m⁻²), $\Sigma nano$ chl a (13.8 ± 1.7 mg chl a m⁻²), and $\Sigma micro$ chl a (6.1 ± 0.9 mg chl a m⁻²) were observed (Plates 1 and 2 and Table 2). Despite relatively high $\Sigma Tchl a$ concentrations, mean ΣPP rates were the lowest estimated when compared to the other regions. Conversely, mean ΣNP rates were the highest (Table 3).

3.2.2. Ionian basin. In the Ionian the MAW is entrained anticyclonically around the stream forming a pool of light less saline water (salinity <38.50) accompanied by high temperatures in the range 14.3–15.5°C (Figure 4). Thus low surface density values characterize this region, forming a well-developed seasonal pycnocline (not shown) separating the water of Atlantic origin from that of Levantine origin at the intermediate layer. This pycnocline limits nutrient upwelling in the euphotic zone, and surface nitrate concentrations were generally low (<0.5 μ M, Plate 1b). Particularly low nitrate concentrations (<0.1 μ M, Plate 1b) were related to the large

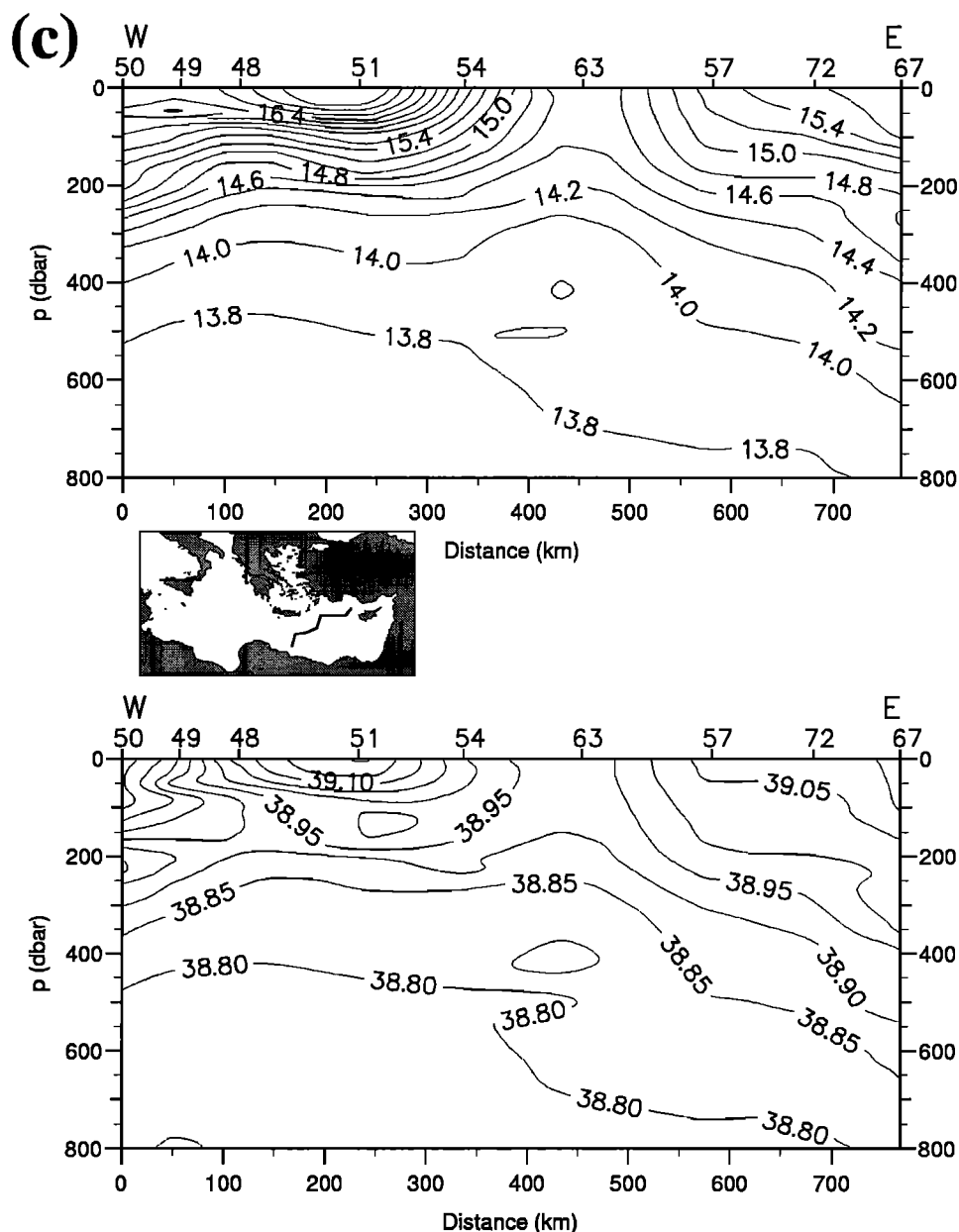


Figure 4. (continued)

Ionian anticyclone (Figure 3), which was also associated with low $\Sigma\text{Tchl } a$ concentrations ($17.3 \pm 1.6 \text{ mg chl } a \text{ m}^{-2}$) and low estimated PP rates ($0.23 \pm 0.03 \text{ g C m}^{-2} \text{ d}^{-1}$) and NP rates ($0.02 \pm 0.01 \text{ g C m}^{-2} \text{ d}^{-1}$, Plates 1c and 3). The concentrations of $\Sigma\text{nano chl } a$ ($9.7 \pm 1.8 \text{ mg chl } a \text{ m}^{-2}$) and $\Sigma\text{micro chl } a$ ($1.7 \pm 0.7 \text{ mg chl } a \text{ m}^{-2}$) observed in this anticyclonic structure were among the lowest measured in the whole eastern basin (Plate 2), whereas $\Sigma\text{pico chl } a$ concentrations were the highest recorded ($5.9 \pm 1.1 \text{ mg chl } a \text{ m}^{-2}$). However, nanophytoplankton always prevailed over picophytoplankton (Plate 2). The second main structure in the Ionian is the doming structure in temperature and salinity (station 26), which is generally indicative of a small-scale cyclonic activity. Associated with this structure, relatively high nitrate and $\Sigma\text{Tchl } a$ concentrations ($1 \mu\text{M}$ and $20.4 \pm 1.0 \text{ mg chl } a \text{ m}^{-2}$, respectively) and estimated ΣPP rate ($0.27 \pm 0.01 \text{ g C m}^{-2} \text{ d}^{-1}$) were found (Plates 1 and 3).

3.2.3. Aegean Sea. The southern Aegean was characterized by a series of cyclonic eddies. A meandering current

seems to advect surface water from the Aegean interior, through the Western Cretan Arc Straits (namely, the Kytherian Straits), into the Cretan passage. It flows eastward south of Crete, while the MMJ transporting MAW is shifted southward close to the African coast. This feature is evident in the satellite image (Plate 1a), which displays two symmetrical cold-core waters indicative of cyclonic eddies at both western and eastern flanks of Crete. The eddies are not so evident in the corresponding objective map (Figure 3) because of the coarse data resolution in this region. In the southern Aegean the averaged $\Sigma\text{Tchl } a$ concentration was similar to the mean calculated for the whole eastern Mediterranean (Table 2). Despite differences in nitrate and $\Sigma\text{Tchl } a$ concentrations (Plate 1), the phytoplankton composition was similar for all the stations: nanophytoplankton (61%) predominated over picophytoplankton (22%) and microphytoplankton (17%).

3.2.4. Levantine basin. The physical and biochemical property distributions changed with the transition from the

Table 2. Phytoplankton Biomass for the Whole Basin and for the Various Regions of the Eastern Mediterranean Sea in Winter^a

Region or Basin	<i>n</i>	Surface, %	Σ Tchl <i>a</i> , mg chl <i>a</i> m ⁻²	Σ pico chl <i>a</i> , mg chl <i>a</i> m ⁻²	Σ nano chl <i>a</i> , mg chl <i>a</i> m ⁻²	Σ micro chl <i>a</i> , mg chl <i>a</i> m ⁻²
Eastern Mediterranean ^b	67	100	20.4	5.4 (27)	12.6 (60)	2.9 (13)
Adriatic Sea	5	8	24.1±2.3	4.2±1.1 (17)	13.8±1.7 (57)	6.1±0.9 (26)
Ionian basin	14	46	19.0±2.9	5.5±1.3 (30)	11.2±2.6 (58)	2.2±0.6 (11)
Aegean Sea	10	11.5	18.8±2.8	4.0±0.9 (22)	11.5±2.3 (61)	3.2±1.0 (17)
Levantine basin	38	34.5	22.1±4.5	5.9±1.5 (27)	13.6±2.8 (62)	2.7±2.0 (12)

^aThe integrated concentration (surface to 1.5 Z_e) is reported for Σ Tchl *a* and for three phytoplankton classes (determined from the pigment-derived criteria): picophytoplankton chl *a* (Σ pico chl *a*), nanophytoplankton chl *a* (Σ nano chl *a*) and microphytoplankton chl *a* (Σ micro chl *a*). Surface refers to the percentage of sea surface covered by each region, and *n* is the number of pigment profiles. Data are presented as the mean ±1 standard deviation. The percentage to Σ Tchl *a* of each phytoplankton class is given in parenthesis.

^bThe average is weighted according to the surface covered by each region.

Ionian to the Levantine basin. To the east of the eastern Cretan passage the near-surface contours (Figure 4) indicated high salinities ranging between 38.85 and 39.0, accompanied by higher temperatures ($\theta > 16^\circ\text{C}$). Thus a frontal system was established in the upper 150–200 m within the interior of the Cretan passage. In the Cretan passage it seems that the pathway of MAW is contrasted by an opposing flow of salty water of Levantine origin. At the entrance of Levantine basin, small packets of MAW ($\theta > 15.5^\circ\text{C}$ and $S < 38.85$) occupied the southernmost portion of the section at stations 50 and 49 in the upper layer of 150 dbar (Figure 4). The hydrographic structures in the Levantine basin, which were better covered by the sampling grid, were (Figure 3 and Plate 1a): (1) the Cretan cyclone, (2) the Rhodes gyre, and (3) the multilobe anticyclone in the southernmost region and along the Egyptian coast (namely, the Mersa-Matruh and the Shikmona gyres). In response to the Cretan cyclone, the broader cyclonic circulation southwest of Crete, relatively high Σ Tchl *a* concentrations were measured (Plate 1c) and relatively high Σ PP and Σ NP rates were estimated (Plate 3). The major hydrographic feature in the Levantine basin is characterized by a broad cyclonic circulation centered over the topographic depression southeast of Rhodes is-

land (i.e., the Rhodes gyre). It extends from the eastern Cretan Arc Straits to the west of Cyprus and includes the West Cyprus cyclonic eddy (Figure 3). This permanent feature [Robinson *et al.*, 1991] is bordered to the north by the westward meandering Asia Minor Current (AMC), while to the south a contrasting system is established by the multilobe anticyclonic circulation. The crescent shape of the Rhodes gyre to the south penetrates into the anticyclonic region. The MAW is found at the left of the section in Figure 4 that corresponds to the southern portion of the Cretan passage (see insert of Figure 4). The most striking feature is represented by the doming of the isotherms and isohalines at station 63 situated at the center of the Rhodes gyre (Figure 4). Its influence encompasses stations 54 and 57, which border the gyre. The center of the gyre is characterized by the relatively cold and less saline water that clearly upwells from the deep layer ($\theta \cong 14.5^\circ\text{C}$ and $S \cong 38.94$). The upwelling transports nitrate into the euphotic layer, which was much higher in the center of the gyre ($\text{NO}_3 = 4 \mu\text{M}$) than at the border or in adjacent areas ($< 1 \mu\text{M}$; see Plate 1b). In the Rhodes gyre the Σ Tchl *a* ($32.9 \text{ mg chl } a \text{ m}^{-2}$) and estimated PP and NP rates (0.42 and $0.15 \text{ g C m}^{-2} \text{ d}^{-1}$, respectively) were among the highest for the whole eastern

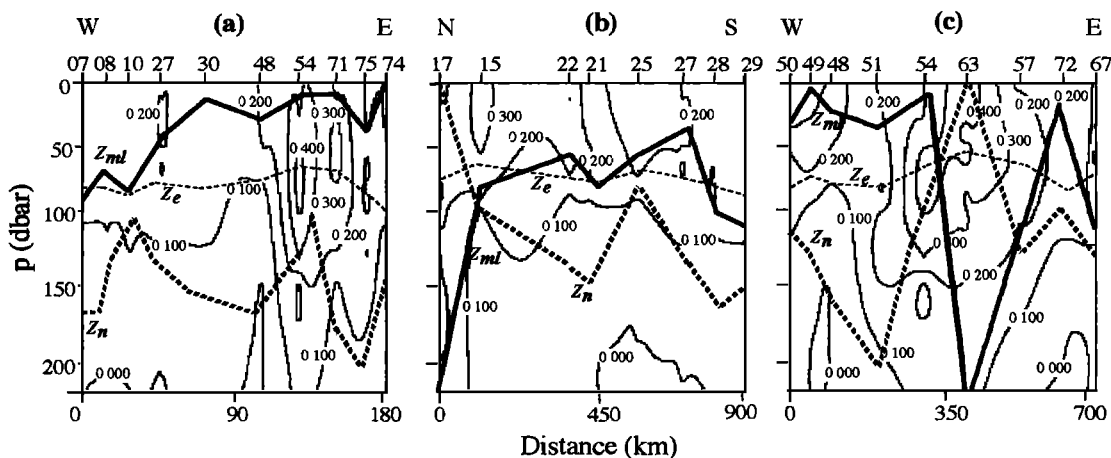


Figure 5. Vertical distribution of Tchl *a* ($\text{mg chl } a \text{ m}^{-3}$) (a) for the cross section through the eastern Mediterranean, (b) for the cross section in the Ionian, and (c) for the cross section in the Levantine basin. Z_e is the depth of the euphotic zone, Z_{ml} is the mixed layer depth, and Z_n is the depth of the nitracline. For the cross sections, see the insert map in Figure 4. The numbers at the top axis indicate the station positions along the section. Note that at stations 17 and 63, Z_{ml} is 475 and 800 m, respectively.

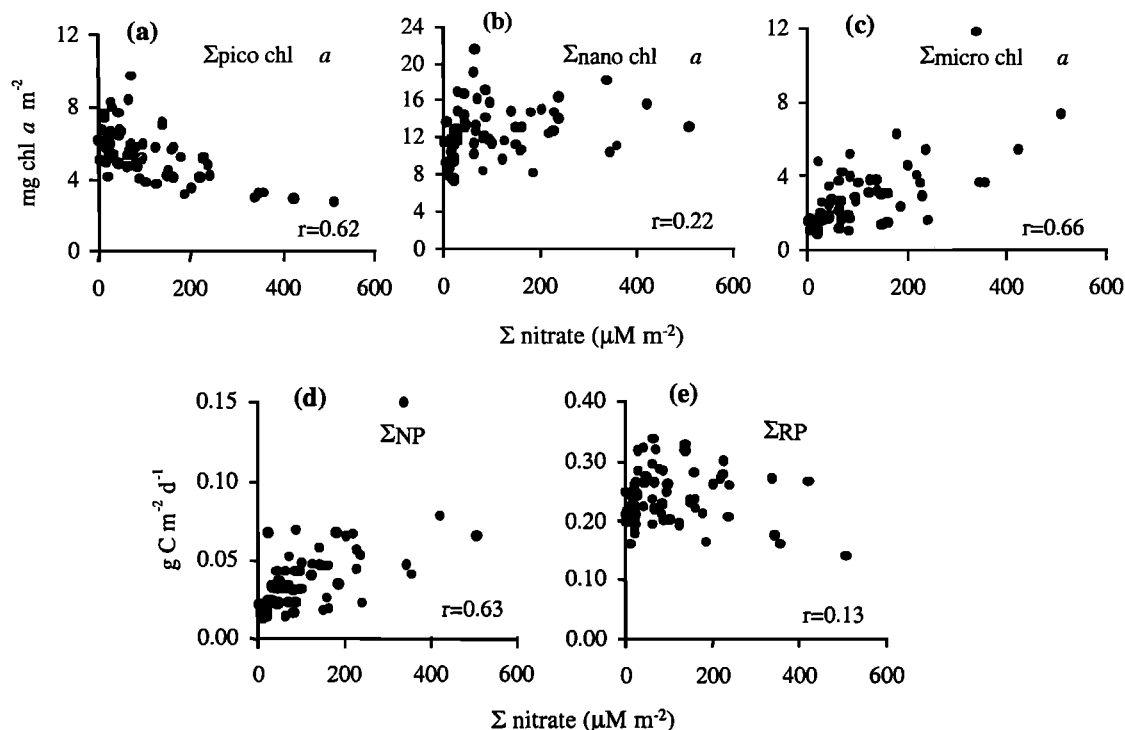


Figure 6. Relationship between nitrate concentrations integrated in the productive layer (Σ nitrate) and concentrations of various biogeochemical indices: (a) Σ pico chl *a* (b) Σ nano chl *a* and (c) Σ micro chl *a* and production rates of (d) Σ NP and (e) Σ RP.

Mediterranean (Plates 1c and 3). These relatively high biomasses were mainly due to microphytoplankton and nanophytoplankton in the center of the gyre, whereas nanophytoplankton and picophytoplankton dominate at the periphery (Plate 2). In contrast, nitrate concentrations in the euphotic zone were $<0.1 \mu\text{M}$ (Plate 1b), and lower $\Sigma\text{Tchl } a$ concentrations as well as estimated ΣPP and ΣNP rates were observed ($17.0 \text{ mg chl } a \text{ m}^{-2}$ and 0.23 and $0.02 \text{ g C m}^{-2} \text{ d}^{-1}$ respectively; Plates 1c and 3) in the southern multilobe anticyclone region (e.g., Shikmona eddy). In this anticyclone the Σ pico chl *a* made an important contribution to the $\Sigma\text{Tchl } a$ (40% $\Sigma\text{Tchl } a$). Conversely, microphytoplankton contributed $<8\%$ to $\Sigma\text{Tchl } a$.

4. Discussion

4.1. General Trends at the Basin Scale

At the basin scale the upper thermocline general circulation in the eastern Mediterranean is dominated by the spreading of MAW (less salty and warmer). This limits nutrient upwelling from deeper to surface layers, and thus the MAW can be considered as the main driving force behind the general oligotrophic character of the whole eastern basin. This view remains valid despite the fact that the nutricline is about 100 m shallower than the previous observations in 1987 because of the general uplifting by the large intrusion of new deep waters at the bottom of the basin [Klein *et al.*, 1999].

The present study confirms the previously reported oligotrophic character of the eastern Mediterranean Sea already reported elsewhere [Berman *et al.*, 1986; Krom *et al.*, 1991; Antoine *et al.*, 1995]. Surface waters were generally nutrient-depleted (Plate 1b), and phytoplankton biomass as

well as estimated primary production rates were low (Plates 1 and 3 and Tables 2 and 3). Moreover, the phytoplankton biomass was essentially dominated by picophytoplankton and nanophytoplankton (87% of $\text{Tchl } a$). As a consequence, new production rates as estimated from the proportion of microphytoplankton (see (8)) were very low. Although our estimates of new production are derived from pigment measurements performed over a 1 month period, and thus mainly reflect the spatiotemporal context of their acquisition, it is tempting to extrapolate these rates of new production to an annual scale for a comparison with previous studies. The estimated value of new production extrapolated to an annual scale ($13.5 \text{ g C m}^{-2} \text{ yr}^{-1}$) is in agreement with the estimation of Béthoux [1989]

Table 3. Estimated Phytoplankton Productions for the Whole Basin and for the Various Region of the Eastern Mediterranean Sea in Winter^a

Region or Basin	<i>n</i>	$\Sigma\text{PP}, \text{ g C m}^{-2} \text{ d}^{-1}$	$\Sigma\text{NP}, \text{ g C m}^{-2} \text{ d}^{-1}$
Eastern Mediterranean ^b	67	0.27	0.04
Adriatic Sea	5	0.24 ± 0.03	0.06 ± 0.01
Ionian Sea	14	0.25 ± 0.04	0.03 ± 0.02
Aegean Sea	10	0.25 ± 0.04	0.04 ± 0.01
Levantine basin	38	0.30 ± 0.05	0.04 ± 0.03

^a The integrated rate (surface to $1.5 Z_e$) is reported for primary (ΣPP), and new production (ΣNP). Data are presented as the mean ± 1 standard deviation, *n* is the number of pigment profiles.

^b The average is weighted according to the surface covered by each region reported in Table 2.

based on deepwater circulation and oxygen budgets ($12 \text{ g C m}^{-2} \text{ yr}^{-1}$). The agreement between these two independent methods validate, at least partly, the pigment-based approach proposed in this study to get estimates of new production from pigment profiles alone. However, our estimate, when converted in terms of nitrogen ($134 \text{ mmol N m}^{-2} \text{ yr}^{-1}$) through the use of a C/N ratio of 106:12.6 proposed for the Mediterranean [Krom *et al.*, 1992], was lower than the $210 \text{ mmol N m}^{-2} \text{ yr}^{-1}$ computed by Krom *et al.* [1992] based on results in the Shikmona gyre. Our estimate and that of Béthoux [1989] could be low because N_2 fixation, potentially significant in the eastern Mediterranean as in other oligotrophic regions [Carpenter, 1983; Olson *et al.*, 1990], is not accounted for in these calculations. Indeed, to explain the unbalanced N budget as well as anomalous N/P ratios in the Mediterranean basin, Béthoux and Copin-Montégut [1986] suggested that N_2 fixation, possibly by cyanobacteria, should be taken into consideration. To our knowledge, there have been no studies devoted to planktonic N_2 fixing organisms (e.g., *Trichodesmium*) for the eastern Mediterranean sea. Therefore the possible role of cyanobacteria in N_2 fixing in the Mediterranean Sea seems to be a crucial point that must be clarified in order to establish a more accurate nitrogen budget of the basin. In addition, our annual estimate of new production does not take into account seasonal variations in chlorophyll, which is the basis of the estimation of primary and new productions in this study. In fact, seasonal variations of PP could be significant in different areas of the eastern Mediterranean as has been reported by Antoine *et al.* [1995]. Antoine *et al.* [1995] showed a twofold increase in the modeled PP during summer, essentially due to the increase in biomass and in PAR during this period.

The observed prevalence of nanophytoplankton and picophytoplankton classes (determined from the pigment-derived criteria) is in agreement with previous studies in Mediterranean waters, which reported the dominance (80-100% of the Tchl *a* biomass) of phytoplankton $<10 \mu\text{m}$ [Raimbault *et al.*, 1988; Li *et al.*, 1993; Yacobi *et al.*, 1995]. Consequently, because protozoa are the main grazers of picophytoplankton and nanophytoplankton [Azam *et al.*, 1993], the microbial food web [Legendre and Rassoulzadegan, 1995; Azam *et al.*, 1983] is likely to be the prevalent trophic pathway in the eastern Mediterranean.

However, the most interesting result is that nanophytoplankton prevail over picophytoplankton. This dominance and ubiquity of nanophytoplankton seems to be a typical characteristic of Mediterranean autotrophic communities [Li *et al.*, 1993; Barlow *et al.*, 1997]. In this sense the communities differ from the phytoplankton communities of "typical" open ocean oligotrophic areas, like the central gyres of oceans, which are generally picophytoplankton-dominated [Goericke and Welschmeyer, 1993; Letelier *et al.*, 1993; Claustre and

Marty, 1995]. In particular, in other oligotrophic areas, prochlorophytes generally account for the larger amount of biomass [Goericke and Welschmeyer, 1993; Letelier *et al.*, 1993; Claustre and Marty, 1995]. In the present study the prochlorophyte contribution, estimated using DV-chl *a* as a unique prochlorophyte marker [Goericke and Repeta, 1992], accounted for only 11% of Tchl *a* (but see later differences at subbasin scale).

To support these observations, we have compared the composition of phytoplankton communities (derived from pigment estimation) in the eastern Mediterranean (this study) to those from monthly estimates at the Hawaii Ocean Time-series (HOT) [Karl and Lukas, 1996] and at the Bermuda Atlantic Time-series (BATS) [Michaels and Knap, 1996] (data available from the U.S. Joint Global Ocean Flux Study data management office, <http://www1.whoi.edu/jgofs>). Stations Aloha in the North Pacific subtropical gyre (study site of HOT) and Bermuda in the North Atlantic (BATS) can be considered as typical oligotrophic areas [Karl and Lukas, 1996; Michaels and Knap, 1996]. Picophytoplankton, nanophytoplankton and microphytoplankton from HOT (from December 1994 to December 1998, 49 profiles, 479 samples) and BATS (from December 1989 to December 1990 and July 1994 to December 1996) databases were determined using the pigment-derived criteria as described in this study (section 2). DV-chl *a* at the HOT site accounted for 40-70% (average 57%) of the Tchl *a*, or about fivefold the average value recorded for the eastern Mediterranean (11%) and 1.6-2.8-fold the higher value measured in the eastern Mediterranean (25% see below). When comparing the average percentage of picophytoplankton, nanophytoplankton and microphytoplankton, picophytoplankton prevailed over nanophytoplankton at the HOT site (63 and 32%, respectively), while both contributed equally at the BATS site (45 and 48%, respectively). Thus these sites appear inherently different from the eastern Mediterranean, where nanophytoplankton were always dominant (60% this study, Tables 2 and 4). Even if the eastern Mediterranean data are compared to data from those periods at BATS when nanophytoplankton were dominant ($>55\%$ of Tchl*a*), picophytoplankton remain relatively more abundant at BATS (average 36%) than in the eastern Mediterranean (average 27%, Table 2).

The general conclusion is therefore that even if the eastern Mediterranean displays a general oligotrophic character (e.g., low biomass and low production rates), it differs from other oligotrophic areas of the world's oceans in terms of its phytoplanktonic composition. The origin of such differences, as well as the potential trophodynamics and biogeochemical implications, remains to be evaluated. In spite of the differences in the phytoplankton composition, average PP and NP rates (0.27 and $0.04 \text{ g C m}^{-2} \text{ d}^{-1}$) were within the range (though near the

Table 4. Comparative Phytoplankton Biomasses and Estimated Primary and New Productions for Cyclonic and Anticyclonic Structures in the Eastern Mediterranean Sea During Winter^a

Structure	$\Sigma\text{Tchl } a,$ $\text{mg chl } a \text{ m}^{-2}$	$\Sigma\text{pico chl } a,$ $\text{mg chl } a \text{ m}^{-2}$	$\Sigma\text{nano chl } a,$ $\text{mg chl } a \text{ m}^{-2}$	$\Sigma\text{micro chl } a,$ $\text{mg chl } a \text{ m}^{-2}$	$\Sigma\text{PP},$ $\text{g C m}^{-2} \text{ d}^{-1}$	$\Sigma\text{NP},$ $\text{g C m}^{-2} \text{ d}^{-1}$
Cyclonic	40.3±15.3	5.5±1.1 (15)	23.3±7.2 (59)	11.5±8.5 (26)	0.31±0.10	0.08±0.05
Anticyclonic	18.8±4.2	7.4±1.5 (40)	10.1±3.5 (53)	1.3±0.4 (7)	0.22±0.03	0.02±0.01
Cyclonic/anticyclonic	2.1	0.7	2.3	8.5	1.4	4.5

^aData are presented as the mean ± 1 standard deviation. The percentage to Tchl *a* is given in parenthesis.

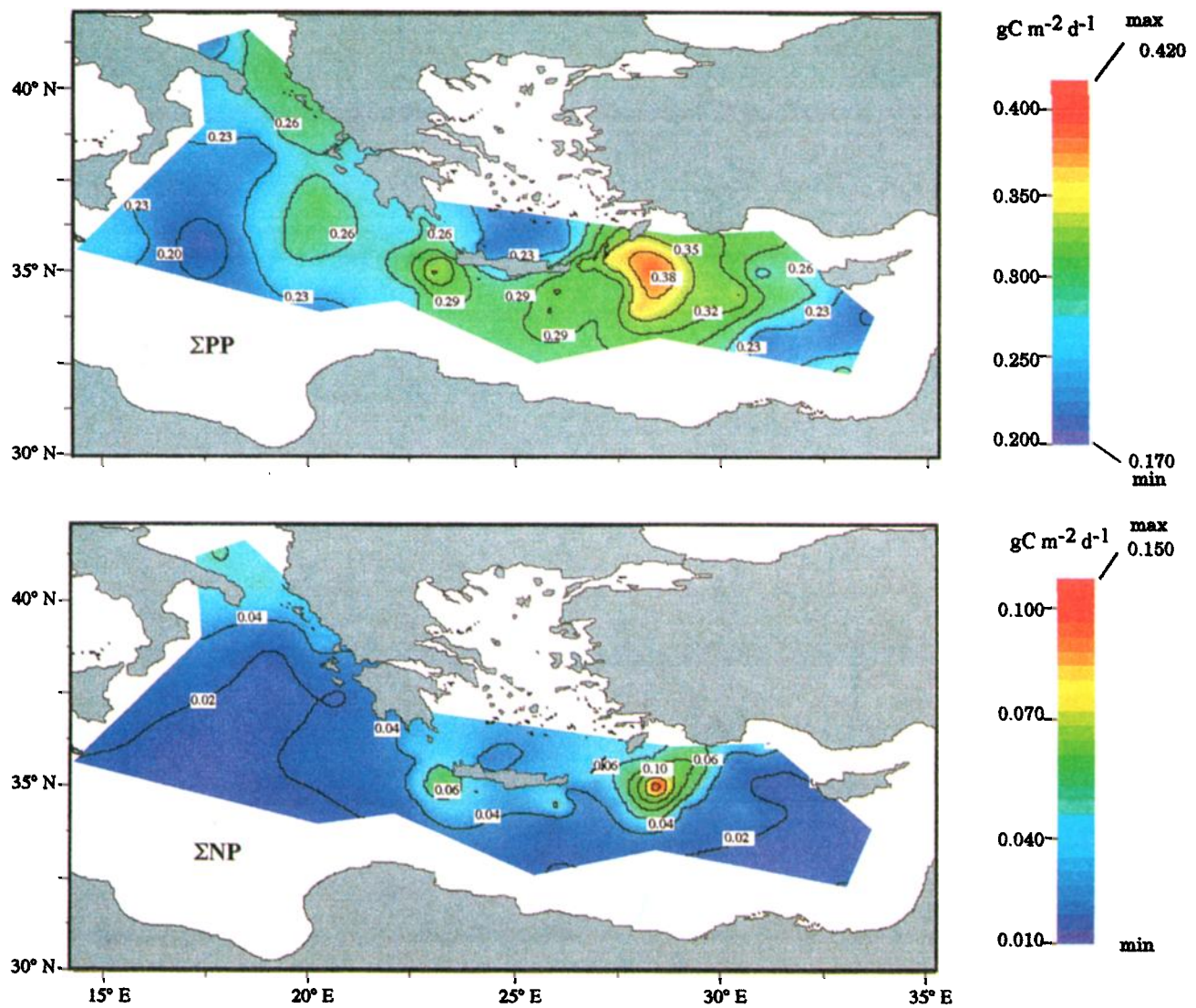


Plate 3. Distribution of estimated (top) ΣPP and (bottom) ΣNP rates in the eastern Mediterranean Sea during winter.

lower end) of previous values (0.22-0.55 and 0.02-0.18 gC m⁻² d⁻¹, respectively) reported for typical oligotrophic areas of the world's oceans [Knauer *et al.*, 1990].

4.2. Variability at the Subbasin Scale and Mesoscale

4.2.1. Cyclonic versus anticyclonic gyres. At the sub-basin scale the oligotrophic character of the eastern Mediterranean Sea can be modified in response to subbasin physical structures. While nutrient concentrations are low in the euphotic zone of the warm anticyclonic gyres, upwelling enriches the euphotic layer of cyclonic gyres with "new" nutrients. In response to the nutrient availability, phytoplankton biomass was 2 times higher in the cyclonic gyres (Adriatic gyre, cyclonic structure in the Ionian basin, Cretan gyre, and Rhodes gyre; Table 4) than in anticyclonic gyres (Ionian and Shikmona gyres). Phytoplankton size classes also responded markedly to this subbasin scale activity. When cyclonic gyres are compared to anticyclonic gyres, the biomass ratio is 8.5, 2, and 0.7 for microphytoplankton, nanophytoplankton, and picophytoplankton, respectively (Table 4). These differences are further illustrated by analyzing the nitrate in the productive layer and the phytoplankton classes pigment-derived relationship (Figure 6). Microphytoplankton were positively related to the surface nitrate concentrations, while the reverse occurred for picophytoplankton. These results are in agreement with previous studies, which demonstrated an association of large species (e.g., microphytoplankton) with eutrophic nitrate-rich areas and small species (e.g., picophytoplankton) with oligotrophic (e.g., nitrate-poor) areas [Malone, 1980; Chisholm, 1992]. As a consequence, an increase in nitrate concentrations is associated with enhanced new production, while regenerated production, which relies on recycled forms of nitrogen, is not related with nitrate levels (Figure 6).

4.2.2. Ionian versus Shikmona gyre. In the Ionian and Shikmona gyres the nitracline was situated below the euphotic zone (the nitracline was, on average, 40 m below Z_e in the Ionian Sea and 70 m below Z_e in the Shikmona gyre, Figure 5) and surface nutrient concentrations were always low or undetectable. Thus, in these anticyclonic structures the general oligotrophic character of the Eastern basin was amplified. ΣTchl *a* concentrations and PP and NP rates were the lowest and the proportion of picophytoplankton was the highest (40% of Tchl *a*, Table 4) of the whole Eastern basin. However, several features indicate differences between both gyres. First, differences recorded in terms of average particulate organic carbon/ΣTchl *a* ratio (429 and 276 for the Shikmona and Ionian gyres, respectively; data not shown) would suggest that the Shikmona gyre is an older system of production with a higher content of non vegetal material (i.e., detritus and/or heterotrophs). Furthermore, a more detailed inspection of the phototrophic prokaryotic community (prochlorophytes and cyanobacteria) revealed differences between the Ionian and the Shikmona gyres. The twofold greater prochlorophyte contribution to Tchl *a* in the Ionian (25% of Tchl *a*) than in the Shikmona gyre (12% of Tchl *a*) and the similar concentrations of zeaxanthin (cyanobacteria and prochlorophytes marker) suggest that prochlorophytes were more abundant in the Ionian, whereas cyanobacteria prevailed in the Shikmona gyre. Because phosphorus depletion is thought to increase from west to east [Krom *et al.*, 1991, and references therein], we speculate that prochlorophytes might be more sensitive to phosphorus limitation than cyanobacteria.

The annual new production rate (36 mmoles N m⁻² yr⁻¹), extrapolated from the estimated daily rates in the Ionian and in the Shikmona gyres using a C/N ratio of 106:12.6 [Krom *et al.*, 1992], is identical to the estimate of Dugdale and Wilkerson [1988] for the whole Eastern basin (36 mmoles N m⁻² yr⁻¹). Dugdale and Wilkerson [1988] made this estimate using an *f* ratio of 0.3 and the primary production measurements performed by Berman *et al.* [1986] in the southeastern Mediterranean. However, these estimations did not take into account seasonal forcing, which may enhance phytoplankton biomass and new production in both the Ionian and Shikmona gyres [Antoine *et al.*, 1995; Krom *et al.*, 1992]. Thus the estimate of Dugdale and Wilkerson [1988] and that of the current study for the two anticyclonic gyres should be considered as minimum values for new production rates in the eastern Mediterranean.

4.2.3. The peculiar case of the Rhodes gyre. In the Rhodes gyre, CTD measurements performed during the study period showed a 800 m mixed layer in the center of the chimney [Malanotte-Rizzoli *et al.*, 1996]. The Tchl *a* content of the 0-230 m (61.3 mg chl *a* m⁻²) layer was 2 times greater than the Tchl *a* content in the productive layer (32.9 mg chl *a* m⁻² in the layer 0-83 m). The relatively high Tchl *a* concentrations (0.2-0.4 mg chl *a* m⁻³) down to 150 m suggest that mixing was active so that the potentially productive biomass is certainly not restricted to the 0-1.5 Z_e layer. In other words, estimates of PP and NP rates in the core of the gyre are probably underestimated. Nevertheless, given these possible underestimations, the average Tchl *a* concentrations at the surface and ΣPP rates computed in the Rhodes gyre were fourfold and twofold higher, respectively, than the values reported by Antoine *et al.* [1995] on the basis of CZCS observations. Two reasons may explain these discrepancies: (1) underestimation of the enhanced Tchl *a* biomass in the Rhodes gyre by CZCS observations during winter convection [Antoine *et al.*, 1995] and (2) interannual variability. Previous studies reported that during cool winters, chlorophyll concentrations were increased as compared to warmer winters [Ediger and Yilmaz, 1996]. In addition, the enhanced Tchl *a* biomass observed can be explained by recent changes in the deep circulation of the eastern Mediterranean [Roether *et al.*, 1996], which might affect the upper thermocline circulation that determines the upwelling of new nutrients in the Rhodes gyre region. We estimate that the Rhodes gyre region, which represents only 10% of the whole Levantine basin, contributed up to 20% of the new production in this basin (Table 5). This result clearly points out the necessity of taking into account small scale features (subbasin and mesoscale) when establishing budgets at a larger scale.

High variability in phytoplankton composition was observed in the Rhodes gyre region. In the core of the gyre the phytoplankton community was dominated by microphytoplankton and nanophytoplankton classes (determined from the pigment-derived criteria). At the border of the gyre, where high biomasses were still recorded (33.5 mg chl *a* m⁻²), nanophytoplankton and picophytoplankton prevailed over microphytoplankton. The upwelling of high-nutrient waters (NO₃ >4.0 μM) in the core of the Rhodes gyre enhanced microphytoplankton biomass, particularly that of diatoms. This group is recognized as the most opportunistic phytoplankton, benefiting from upwelling and active mixing [Fogg, 1991]. The occurrence of a bloom of nanophytoplankton and picophytoplankton, in the vicinity of the gyre, is a rather unusual phenomenon.

Table 5. Biogeochemical Significance of the Rhode Gyre Region in the Levantine Basin During Winter

	Area, 10 ¹² m ²	ΣNP, g C m ⁻² d ⁻¹	ANP, ^a 10 ¹² g C d ⁻¹
Rhodes gyre region	0.060 ^b	0.071	0.004
Levantine basin	0.511 ^c	0.031	0.016

^aANP is the areal or basin daily new production.

^bCalculated on the basis of a rectangular surface where one side is the distance latitude between stations 61 and 54 and the other side is the distance longitude between stations 62 and 68.

^cExcluded the Rhodes gyre region and case 2 waters [see Antoine *et al.*, 1995].

High biomasses of nanophytoplankton have been reported associated with peculiar hydrodynamic conditions in association with a geostrophic front in the western Mediterranean [e.g., *Claustre et al.*, 1994]. Similarly, mesoscale activity in the vicinity of the Rhodes gyre might be the origin of similar conditions.

5. Conclusions

Phytoplankton composition and primary production measurements in the eastern Mediterranean are very sparse and generally restricted to particular regions (e.g., the Shikmona gyre) [Krom *et al.*, 1992]. To our knowledge the only basin-wide study in the eastern Mediterranean is restricted to chlorophyll and primary production derived from ocean color (CZCS) data [Antoine *et al.*, 1995]. The study presented here is by far the most complete basin-wide survey of phytoplankton biomass and composition in the eastern Mediterranean, in particular, in the Ionian and Levantine basins.

From the distribution of phytoplankton biomass and new production it is clear that the eastern Mediterranean is not a homogenous oligotrophic water body. Although significant differences at small scales (subbasin scale and mesoscale) were documented during this study, two main zones can be recognized in the eastern Mediterranean basin. These correspond to the separation of the basin by the modified Atlantic water current, a northern zone (north of the 35th to 38th parallels), which is dominated by cyclonic circulation, and a southern zone which is dominated by anticyclonic structures. Therefore relatively high phytoplankton standing stocks and new production are confined in the northern zone, while the oligotrophic character increases in the southern zone, where biomasses and new production are particularly low.

Our estimate of the annual new production of the eastern Mediterranean is in agreement with that calculated previously using an independent method [e.g., *Béthoux*, 1989]. This result validates, at least partially, the pigment-based method coupled with the modeling of primary production for the retrieval of new production. Nevertheless, further work is needed to cross compare such estimates and those derived from ¹⁵N incubation techniques. Similarly, the importance of N₂ fixation and its potential influence on biogeochemical cycling in the eastern Mediterranean Sea deserves attention.

Acknowledgments. This study was funded by the European Commission under MAST-MTP-I-GEODYME (contract n° MAS2-CT93-0061), MAST-MTP-II-MATER (contract n° MAS3-CT96-0051) and PROMOLEC (contract n° MAS3-CT97-0128). Financial

support from "Direction des Relations Internationales of CNRS", "Réseau diversité marine", and the PROSOPE operation from the PROOF-France Program are acknowledged. We thank W. Roether, chief scientist for *Meteor* cruise 31/1, and the captain and the crew of R/V *Meteor* for their continued support during the 1995 cruise. We are particularly grateful to J.-P. Béthoux, coordinator of the GEODYME project, for supporting this study. We are grateful to A. Dickson and the three anonymous reviewers for constructive comments. D. Antoine is particularly acknowledged for PP computation, P. Lee and R. Whitehead are acknowledged for English corrections, and J.-P. Chanut is acknowledged for help in statistics. F.V. was supported by an EEC grant (MAS2-CT-94-5027).

References

- Andersen, R. A., G. W. Sunders, M. P. Paskind, and J. P. Sexton, Ultrastructure and 18S rRNA gene sequence for *Pelagomonas calceolata* nov. gen. et spec. nov. and the description of a new algal class, the Pelagophyceae classis nov., *J. Phycol.*, 29, 701-715, 1993.
- Antoine, D., A. Morel, and J.-M. André, Algal pigment distribution and primary production in the eastern Mediterranean as derived from Coastal Zone Color Scanner observations, *J. Geophys. Res.*, 100, 16,193-16,209, 1995.
- Arpin, N., W. A. Svec, and S. Liaaen-Jensen, A new fucoxanthin-related carotenoid from *Coccolithus huxleyi*, *Phytochemistry*, 15, 529-532, 1976.
- Azam, F., T. Fenchel, J. G. Field, J. S. Gray, L. A. Meyer-Reil, and F. Thingstad, The ecological role of water-column microbes in the sea, *Mar. Ecol. Prog. Ser.*, 10, 257-263, 1983.
- Barlow, R. G., R. F. C. Mantoura, D. G. Cummings, and T. W. Fileman, Pigment chemotaxonomic distributions of phytoplankton during summer in the western Mediterranean, *Deep Sea Res., Part II*, 44, 833-850, 1997.
- Berman, T., Y. Azov, A. Schneller, P. Valline, and D.W. Townsend, Extent, transparency, and phytoplankton distribution of the neritic waters overlying the Israeli coastal shelf, *Oceanol. Acta*, 9, 439-447, 1986.
- Béthoux, J.P., Oxygen consumption, new production, vertical advection and environmental evolution in the Mediterranean sea, *Deep Sea Res., Part I*, 36, 769-781, 1989.
- Béthoux, J.P., and G. Copin-Montegut, Biological fixation of atmospheric nitrogen in the Mediterranean Sea, *Limnol. Oceanogr.*, 31, 1353-1358, 1986.
- Béthoux, J.-P., and B. Gentili, The Mediterranean Sea, a test area for marine and climatic interactions, in *Ocean Processes in Climate Dynamics: Global and Mediterranean Examples*, edited by A. R. Robinson, and P. Malanotte-Rizzoli, pp. 239-254, Kluwer, Norwell, Mass., 1994.
- Bjørnland, T., and S. Liaaen-Jensen, Distribution pattern of carotenoids in relation to chromophyte phylogeny and systematics, in *The Chromophyte Algae: Problems and Perspectives*, edited by G. C. Geen, B. S. C. Leaderbeater, and W. L. Diver, pp. 37-60, Clarendon, Oxford, England, U. K., 1989.
- Bjørnland, T., S. Liaaen-Jensen, and J. Throndsen, Carotenoids of the marine chrysophyte *Pelagococcus subviridis*, *Phytochemistry*, 28, 3347-3353, 1989.
- Carpenter, E. J., and D. G. Capone, *Nitrogen in the Marine Environment*, Academic, San Diego, Calif., 1983.
- Carther, E. F., and A. R. Robinson, Analysis models for the estimation of ocean fields, *J. Atmos. Oceanic Technol.*, 4, 49-74, 1987.
- Chavez, F. P., K. R. Buck, S. K. Service, J. Newton, and R. T. Barber, Phytoplankton variability in the central and eastern tropical Pacific, *Deep Sea Res., Part II*, 43, 835-870, 1996.
- Chisholm, S. W., Phytoplankton size, in *Primary Productivity and Biogeochemical Cycles in the Sea*, edited by P. G. Falkowski and A. D. Woodhead, pp. 213-217, Plenum, New York, 1992.
- Chisholm, S. W., R. J. Olson, E. R. Zettler, R. Goericke, J. B. Waterbury, and N. A. Welschmeyer, A novel free-living prochlorophyte abundant in the oceanic euphotic zone, *Nature*, 334, 340-344, 1988.
- Claustre, H., The trophic status of various oceanic provinces as revealed by phytoplankton pigment signatures, *Limnol. Oceanogr.*, 39, 1206-1210, 1994.
- Claustre, H., and J.-C. Marty, Specific phytoplankton biomasses and

- their relation to primary production in the tropical North Atlantic, *Deep Sea Res., Part I*, 42, 1475-1493, 1995.
- Claustre, H., P. Kerhervé, J.-C. Marty, L. Prieur, C. Videau, and J.-H. Heccq, Phytoplankton dynamics associated with a geostrophic front: Ecological and biogeochemical implications, *J. Mar. Res.*, 52, 711-742, 1994.
- Dugdale, R. C., and F. P. Wilkerson, Nutrient sources and primary production in the eastern Mediterranean, *Oceanol. Acta*, 9, 179-184, 1988.
- Ediger, D., and A. Yilmaz, Characteristics of deep chlorophyll maximum in the northeastern Mediterranean with respect to environmental conditions, *J. Mar. Syst.*, 9, 291-303, 1996.
- Eppley, R. W., and B. J. Peterson, Particulate organic matter flux and planktonic new production in the deep ocean, *Nature*, 282, 677-680, 1979.
- Fogg, G. E., The phytoplankton way of life, *J. Phycol.*, 118, 191-232, 1991.
- Gieskes, W. W. C., and G. W. Kraay, Unknown chlorophyll *a* derivatives in the North Sea and the tropical Atlantic Ocean revealed by HPLC analysis, *Limnol. Oceanogr.*, 28, 757-766, 1983a.
- Gieskes, W. W. C., and G. W. Kraay, Dominance of Cryptophyceae during the phytoplankton spring bloom in the central North Sea detected by HPLC analysis of pigments, *Mar. Biol.*, 75, 179-185, 1983b.
- Gieskes, W. W. C., G. W. Kraay, A. Nontji, D. Setiapermana, and D. Sutomo, Monsoonal alternation of a mixed and a layered structure in the euphotic zone of the Banda Sea (Indonesia): A mathematical analysis of algal pigment fingerprints, *Neth. J. Sea Res.*, 22, 123-137, 1988.
- Goericke, R., and D.J. Repeta, The pigments of *Prochlorococcus marinus*: The presence of divinyl chlorophyll *a* and *b* in a marine prokaryote, *Limnol. Oceanogr.*, 37, 425-433, 1992.
- Goericke, R., and D.J. Repeta, Chlorophylls *a* and *b* and divinyl-chlorophylls *a* and *b* in the open subtropical North Atlantic Ocean, *Mar. Ecol. Prog. Ser.*, 101, 307-313, 1993.
- Goericke, R., and N. A. Welschmeyer, The marine prochlorophyte *Prochlorococcus* contributes significantly to phytoplankton biomass and primary production in the Sargasso sea, *Deep Sea Res., Part I*, 40, 2283-2294, 1993.
- Goldman, J., Potential role of large oceanic diatoms in new primary production, *Deep Sea Res., Part I*, 40, 159-168, 1993.
- Grasshoff, K., M. Erhardt, and K. Kremling (Eds.), *Methods of Seawater Analysis*. Verlag-Chemie, Weinheim, Germany, 1983.
- Guillard, R. R. L., L. S. Murphy, P. Foss, and S. Liaaen-Jensen, *Synechococcus* spp. as likely zeaxanthin dominant ultraphytoplankton in the north Atlantic, *Limnol. Oceanogr.*, 30, 412-414, 1985.
- Hooks, C. E., R. R. Bidigare, M. D. Keller, and R. R. L. Guillard, Coccolid eukaryotic marine ultraplankters with four different HPLC pigment signatures, *J. Phycol.*, 24, 571-580, 1988.
- Jeffrey, S. W., A report of green algal pigments in the central North Pacific Ocean, *Mar. Biol.*, 37, 33-37, 1976.
- Jeffrey, S. W., and M. Vesik, Introduction to marine phytoplankton and their pigment signatures, in *Phytoplankton Pigments in Oceanography*, edited by S. W. Jeffrey, R. F. C. Mantoura, and S. W. Wright, pp. 407-428, U. N. Educ., Sci., and Cult. Org., Paris, 1997.
- Jeffrey, S. W., M. Sielicki, and F.T. Haxo, Chloroplast pigment patterns in dinoflagellates, *J. Phycol.*, 11, 374-385, 1975.
- Johansen, J. E., W. A. Svec, S. Liaaen-Jensen, and F. T. Haxo, Carotenoids of the Dinophyceae, *Phytochem.*, 13, 2261-2271, 1974.
- Kana, T. M., and P. M. Glibert, Effect of irradiances up to 2000 $\mu\text{E m}^{-2} \text{s}^{-1}$ on marine *Synechococcus* WH7803-I: Growth, pigmentation and cell composition, *Deep Sea Res., Part I*, 34, 479-495, 1987.
- Karl, D. M., and R. Lukas, The Hawaii Ocean Time-series (HOT) program: Background, rationale and field implementation, *Deep Sea Res., Part II*, 43, 129-156, 1996.
- Kimor, B., T. Berman, and A. Schneller, Phytoplankton assemblages in the deep chlorophyll maximum layers off the Mediterranean coast of Israel, *J. Plankton Res.*, 9, 433-443, 1987.
- Klein, B., W. Roether, B. B. Manca, D. Bregant, V. Beitzl, V. Kovacevic and A. Luchetta, The large deep water transient in the eastern Mediterranean, *Deep Sea Res., Part I*, 46, 371-414, 1999.
- Knauer, G. A., D. G. Redalje, W. G. Harrison, and D. M. Karl, New production at the VERTEX time-series site, *Deep Sea Res., Part A*, 37, 1121-1134, 1990.
- Krom, M. D., N. Kress, S. Brenner, and L. I. Gordon, Phosphorus limitation of primary productivity in the eastern Mediterranean Sea, *Limnol. Oceanogr.*, 36, 424-432, 1991.
- Krom, M. D., S. Brenner, N. Kress, A. Neori, and L. I. Gordon, Nutrients dynamics and new production in warm-core eddy from the eastern Mediterranean Sea, *Deep Sea Res., Part A*, 39, 467-480, 1992.
- Legendre, L., and S. Demers, Towards dynamic biological oceanography and limnology, *Can. J. Fish. Aquat. Sci.*, 41, 2-19, 1984.
- Legendre, L., and J.-L. LeFevre, Hydrodynamical singularities as controls of recycled versus export production in oceans, in *Productivity of the ocean: present and past*, edited by W. H. Berger, V. S. Smatacek, and G. Wefer, pp. 49-63, John Wiley, New York, 1989.
- Legendre, L., and F. Rassoulzadegan, Plankton and nutrient dynamics in coastal waters, *Ophelia*, 41, 153-172, 1995.
- Letelier, R. M., R. R. Bidigare, D. V. Hebel, M. Ondrusek, C. D. Winn, and D. M. Karl, Temporal variability of phytoplankton community structure based on pigment analysis, *Limnol. Oceanogr.*, 38, 1420-1437, 1993.
- Li, W. K. W., T. Zohary, Y. Z. Yacobi, and A. M. Wood, Ultraphytoplankton in the eastern Mediterranean Sea: towards deriving phytoplankton biomass from flow cytometric measurements of abundance, fluorescence and light scatter, *Mar. Ecol. Prog. Ser.*, 102, 79-87, 1993.
- Lohrenz, S. E., J. J. Cullen, D. A. Phinney, D. P. Olson, and C. S. Yentsch, Distribution of pigments and primary production in a Gulf Stream meander, *J. Geophys. Res.*, 98, 14,545-14,560, 1993.
- Malanotte-Rizzoli, P., et al., Experiment in eastern Mediterranean probes origin of deep water masses, *Eos, Trans. AGU*, 77, 305-311, 1996.
- Malanotte-Rizzoli, P., et al., A synthesis of the Ionian Sea hydrography, circulation and water mass pathways during POEM-Phase I, *Prog. Oceanogr.*, 39, 153-204, 1997.
- Malone, T. C., Algal size, in *The Physiological Ecology of Phytoplankton*, edited by I. Morris, pp. 433-463, Univ. of Calif., Berkeley and Los Angeles, 1980.
- Mann, K. H., and J. R. N. Lazier, *Dynamics of Marine Ecosystems: Biological-Physical Interactions in the Oceans*, Blackwell Sci., Malden, Mass., 1991.
- Mantoura, R. F. C., and D. Repeta, Calibration methods for HPLC, in *Phytoplankton pigments in oceanography*, edited by S. W. Jeffrey, R. F. C. Mantoura, and S. W. Wright, pp. 407-428, U. N. Educ., Sci., and Cult. Org., Paris, 1997.
- Michaels, A. F., and A. Knap, Overview of the U.S. JGOFS Bermuda Atlantic time-series study and Hydrostation S program, *Deep Sea Res., Part II*, 43, 157-198, 1996.
- Michaels, A. F., and M. W. Silver, Primary production, sinking fluxes and the microbial food web, *Deep Sea Res., Part A*, 35, 473-490, 1988.
- Moore, L. R., R. Goericke, and S. W. Chisholm, Comparative physiology of *Synechococcus* and *Prochlorococcus*: Influence of light and temperature on growth, pigments, fluorescence and absorptive properties, *Mar. Ecol. Prog. Ser.*, 116, 259-275, 1995.
- Morel, A., Optical modeling of the upper ocean in relation to its biogenous matter content (case I waters), *J. Geophys. Res.*, 93, 10,749-10,768, 1988.
- Morel, A., Light and marine photosynthesis: A spectral model with geochemical and climatological implications, *Prog. Oceanogr.*, 26, 301-342, 1991.
- Morel, A., D. Antoine, M. Babin, and Y. Dandonneau, Measured and modeled primary production in the northeast Atlantic (EUMELI JGOFS program): The impact of natural variations in photosynthetic parameters on model predictive skill, *Deep Sea Res., Part I*, 43, 1273-1304, 1996.
- Olson, R. J., S. W. Chisholm, E. R. Zettler, M. A. Altabet, and J. A. Dusenberry, Spatial and temporal distributions of prochlorophyte picoplankton in the north Atlantic ocean, *Deep Sea Res., Part A*, 37, 1033-1051, 1990.
- Ozsoy, E., A. Hecht, U. Unluata, S. Brenner, H. I. Sur, J. Bishop, M. A. Latif, Z. Rozentraub, and T. Oguz, A synthesis of the Levantine basin circulation and hydrography, 1985-1990, *Deep Sea Res., Part II*, 40, 1075-1120, 1993.
- Partensky, F., N. Hoepffner, W. K. W. Li, O. Ulloa, and D. Vaultot, Photoacclimation of *Prochlorococcus* sp. (Prochlorophyta)

- stains isolated from the North Atlantic and the Mediterranean Sea, *Plant Physiol.*, *101*, 285-296, 1993.
- POEM Group, General circulation of the eastern Mediterranean, *Earth Sci. Rev.*, *32*, 285-309, 1992.
- Raimbault, P., I. Taupier-Letage, and M. Rodier, Vertical size distribution of phytoplankton in the western Mediterranean Sea during early summer, *Mar. Ecol. Prog. Ser.*, *45*, 153-158, 1988.
- Repeta, D. J., and T. Bjornland, Preparation of carotenoid standards, in *Phytoplankton Pigments in Oceanography* edited by S. W. Jeffrey, R. F. C. Mantoura, and S. W. Wright, pp. 239-260, U. N. Educ., Sci., and Cult. Org., Paris, 1997.
- Robinson, A. R., M. Golnaraghi, W. G. Leslie, A. Artegiani, A. Hecht, E. Lazzone, A. Michelato, E. Sansone, A. Theocharis, and U. Unluata, Structure and variability of the eastern Mediterranean general circulation, *Dyn. Atmos. Oceans*, *15*, 215-240, 1991.
- Roether, W., B. Manca, B. Klein, D. Bregant, D. Georgopoulos, V. Beitzel, V. Kovacevic, and A. Luchetta, Recent changes in eastern Mediterranean deep waters, *Science*, *271*, 333-335, 1996.
- Salihoglu, I., C. Saydam, Ö. Bastürk, K. Yılmaz, D. Göçmen, E. Hatipoğlu, and A. Yılmaz, Transport and distribution of nutrients and chlorophyll *a* by mesoscale eddies in the northeastern Mediterranean, *Mar. Chem.*, *29*, 375-390, 1990.
- Sieburth, J., V. Smetacek, and J. Lenz, Pelagic ecosystem structure: Heterotrophic compartments of the plankton and their relationship to plankton size fractions, *Limnol. Oceanogr.*, *23*, 1256-1263, 1978.
- Simon, N., R. G. Barlow, D. Marie, F. Partensky, and D. Vaultot, Characterization of oceanic photosynthetic picoeukaryotes by flow cytometry, *J. Phycol.*, *30*, 922-935, 1994.
- Theocharis, A., D. Georgopoulos, A. Lascaratos, and K. Nittis, Water masses and circulation in the central region of the eastern Mediterranean: Eastern Ionian, South Aegean and Northwest Levantine, 1986-1987, *Deep Sea Res., Part II.*, *40*, 1121-1142, 1993.
- United Nations Educational, Scientific, and Cultural Organisation, Algorithms for computations of fundamental properties of seawater, *Tech. Pap. Mar. Sci.*, *44*, 53 pp., 1983.
- Vidussi, F., H. Claustre, J. Bustillos-Guzman, C. Cailliau, and J.-C. Marty, Determination of chlorophylls and carotenoids of marine phytoplankton: Separation of chlorophyll *a* from divinyl-chlorophyll *a* and zeaxanthin from lutein, *J. Plankton Res.*, *18*, 2377-2382, 1996.
- Villareal, T. A., C. Pilska, M. Brzezinski, F. Lipschultz, M. Dennett, and G. B. Gardner, Upward transport of oceanic nitrate by migrating diatom mats, *Nature*, *397*, 423-425, 1999.
- Wright, S. W., and S. W. Jeffrey, Fucoxanthin pigment markers of marine phytoplankton analysed by HPLC and HPTLC, *Mar. Ecol. Prog. Ser.*, *38*, 259-266, 1987.
- Yacobi, Y. Z., T. Zohary, N. Kress, A. Hecht, R. D. Robarts, M. Waiser, A.M. Wood, and W. K. W. Li, Chlorophyll distribution throughout the southeastern Mediterranean in relation to the physical structure of the water mass, *J. Mar. Syst.*, *6*, 179-190, 1995.

H. Claustre, J.-C. Marty, and F. Vidussi, Observatoire Océanologique de Villefranche, Laboratoire d'Océanographie de Villefranche, Université Pierre et Marie Curie and CNRS/INSU, B. P. 08, quai de la Darse, 06238 Villefranche-sur-mer, France. (claustre@obs-vmfr.fr; marty@obs-vmfr.fr; fvidussi@wanadoo.fr)

A Luchetta, Istituto Talassografico, viale R. Gessi 2, 34123 Trieste, Italy. (luchetta@itt.ts.cnr.it)

B. B. Manca, Istituto Nazionale di Oceanografia e Geofisica Sperimentale, Borgo Grotta Gigante 42/c, 34010 Sgonico, Trieste, Italy. (bmanca@ogs.trieste.it).

(Received April 27 1999; revised March 26, 2001; accepted March 26, 2001)